20. PETROLOGY AND GEOCHEMISTRY OF VOLCANIC ROCKS, DSDP LEG 55, EMPEROR SEAMOUNT CHAIN

R. James Kirkpatrick, Department of Geology, University of Illinois, Urbana, Illinois
David A. Clague, Department of Geology, Middlebury College, Middlebury, Vermont
and
Walter Freisen, U. S. Geological Survey, Menlo Park, California

INTRODUCTION

The volcanic rocks recovered on Deep Sea drilling Project Leg 55 from the central Emperor Seamount chain in the northwest Pacific were all erupted subaerially, and include tholeiitic basalts, tholeiitic picrites alkali basalts, and hawaiites similar to those found in the southern Emperor chain and the Hawaiian chain. These rocks were recovered from three sites (430, 432, and 433) on three different seamounts along the Emperor chain (Figure 1). The purposes of this paper are to present our post-cruise petrographic and geochemical data, to classify the rock types, to discuss the chemical stratigraphy of the volcanics, to discuss the petrogenetic relationships at each site, to discuss the variation in basalt composition along the chain, and to discuss the origin of linear island chain basalts. The shipboard petrographic and chemical data, coring and recovery information, and the flow by flow stratigraphy are presented in the appropriate site chapters (Leg 55 Scientific Party, this volume) and in the Introduction and Synthesis (Jackson et al., this volume). These chapters also present the rationale and operational history of Leg 55.

The modal petrographic data to be presented here were obtained using normal point-counting techniques. The chemical analyses were done in the USGS analytical laboratory in Menlo Park, California. Most were done using XRF techniques. A comparison of XRF and wet chemical analyses of four samples is presented in Table 1. The two kinds of analyses give similar results, except for MgO, for which the XRF analyses are higher by about 0.2 weight per cent. Although no samples were analyzed both at Menlo Park and on board, the more numerous analyses done on board the *Challenger* also appear to be comparable to the USGS analyses, and all available analyses will be used here. Whole-rock electron microprobe analyses of fused glasses made from some of the same samples reported here are given by Bence et al. (this volume). Electron microprobe analyses of phenocryst and groundmass olivine, pyroxene, plagioclase, iron-titanium oxides, and chrome spinels are given by Clague et al. (this volume). Electron microprobe analyses of clay minerals in the samples dated by K/Ar techniques are presented by Dalrymple et al. (this volume).

SITE 430

Site 430 was drilled into a lagoonal sediment pond near the center of Ōjin Seamount at 37°59.24′N, 170° 35.86′E. Hole 430A is the only hole to reach the volcanic sequence. Five lava flows were penetrated in the 28 meters of basement drilled. The top four flows are aphyric to very sparsely olivine and plagioclase phyric hawaiites. The fifth (bottom) flow is a plagio-

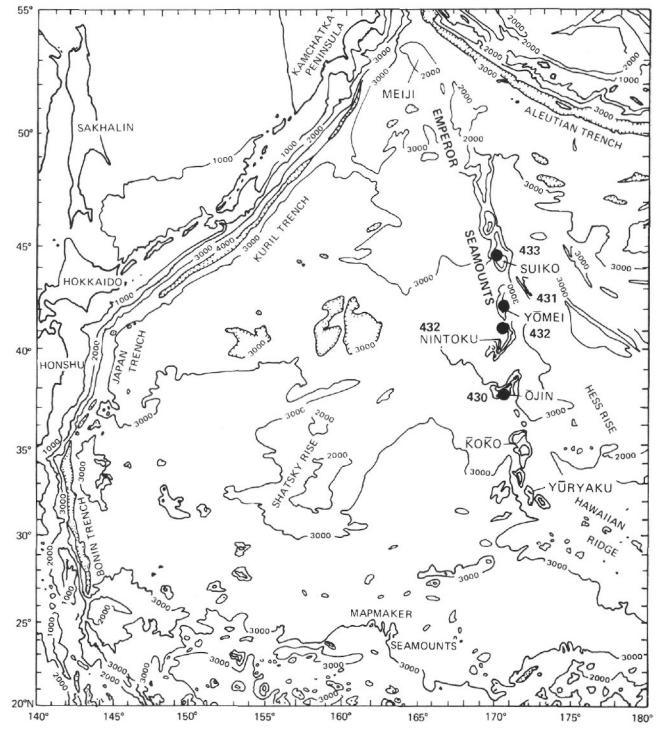

Figure 1. *Locations of Leg 55 Sites.*

TABLE 1
Comparison of Wet-Chemical and X-ray Fluorescence Analyses on Four Samples of Lava Flows Recovered on DSDP Leg 55.[a]

Hole	430A		433A		433C		433C	
Core-Section, Interval (cm)	4-2, 110–113		21-4, 129–138		15-6, 16–31		17-1, 78–82	
Type	Wet	X-ray	Wet	X-ray	Wet	X-ray	Wet	X-ray
SiO_2	49.35	49.49	48.08	47.79	49.03	48.78	49.75	49.45
Al_2O_3	17.55	17.58	15.11	15.05	14.29	14.54	14.02	14.14
FeO	12.62	12.51	13.95	14.01	12.97	13.00	13.05	13.10
MgO	2.90	3.07	5.13	5.40	6.74	6.83	6.29	6.52
CaO	6.17	6.10	9.36	9.48	10.64	10.59	10.70	10.67
Na_2O	4.63	4.48	3.61	3.60	2.95	2.96	2.83	2.88
K_2O	2.06	2.05	0.95	0.91	0.28	0.25	0.34	0.29
TiO_2	3.31	3.32	3.19	3.23	2.64	2.61	2.55	2.51
P_2O_5	1.35	1.33	0.43	0.35	0.30	0.28	0.29	0.25
MnO	0.06	0.07	0.19	0.18	0.17	0.16	0.19	0.19
Totals	100.00	100.00	100.00	100.00	100.00	100.00	100.00	100.00

[a]The analyses have been dry reduced and normalized to 100 per cent for direct comparison.

clase and olivine phyric tholeiitic basalt of which only two pieces were recovered.

Chemistry

Chemically, the volcanic rocks recovered at Site 430 are similar to Hawaiian-type hawaiites and tholeiitic basalts (Macdonald, 1968). Table 2 presents the post-cruise major-element analyses, both as received and dry-reduced, along with CIPW norms assuming $Fe^{+3}/Fe^{+3} + Fe^{+2} = 0.15$. Table 3 presents the post-cruise trace-element analyses. Figure 2 presents a diagram of total alkalis versus silica for all Leg 55 volcanic rocks. Figure 3 presents MgO variation diagrams for the Site 430 analyses, including both the shipboard and post-cruise data. Figure 4 presents the stratigraphic variation for each of the analyzed elements.

It is clear from the plot of total alkalis versus silica and the MgO variation diagrams that the hawaiites and the tholeiitic basalt are distinctly different rocks and cannot be related to each other, at least by low-pressure processes. The hawaiite flows, on the other hand, are very similar to each other. For most elements, the variation within Flow 1 is as large as or larger than variation between the flows. The hawaiites all have very similar

TABLE 2
Chemical Analyses and Norms of Volcanic Rocks from Hole 430A, Ōjin Seamount

Core-Sec., Interval (cm)	4-2, 110–118	5-1, 21–27	5-2, 102–115	6-1, 17–25	6-3, 52–63	6-4, 7–15	6-4, 140–150
Flow Unit	1	1	1	3	3	4	5
				As Received			
SiO_2	47.06	47.60	48.11	48.33	47.80	48.03	47.66
Al_2O_3	16.72	15.88	15.53	15.80	16.18	15.42	15.29
Fe_2O_3	10.76	10.08	5.14	7.61	8.02	6.71	4.54
FeO	2.21	2.84	6.62	3.98	4.03	4.85	7.91
MgO	2.92	3.24	4.58	3.82	3.87	4.45	5.63
CaO	5.80	6.61	6.84	7.14	6.58	6.69	10.98
Na_2O	4.26	4.29	4.08	4.34	4.30	4.26	3.00
K_2O	1.95	1.68	1.53	1.60	1.68	1.60	0.36
H_2O^+	1.23	1.02	1.53	0.94	1.17	1.53	0.39
H_2O^-	2.54	2.17	1.65	2.16	2.20	2.06	1.01
TiO_2	3.16	3.06	2.92	2.92	2.88	2.73	2.76
P_2O_5	1.26	1.18	1.13	1.22	1.24	1.26	0.30
MnO	0.07	0.07	0.13	0.09	0.11	0.13	0.18
CO_2	0.11	0.10	0.03	0.03	0.05	0.04	0.04
Total (%)	100.05	99.82	99.82	99.98	100.11	99.76	100.05
				Dry Reduced Normalized			
SiO_2	49.49	49.83	50.06	50.30	49.85	50.31	48.56
Al_2O_3	17.58	16.62	16.16	16.44	16.87	16.15	15.58
FeO	12.51	12.47	11.70	11.27	11.73	11.41	12.22
MgO	3.07	3.39	4.77	3.98	4.04	4.66	5.74
CaO	6.10	6.92	7.12	7.43	6.86	7.01	11.19
Na_2O	4.48	4.49	4.25	4.52	4.48	4.46	3.06
K_2O	2.05	1.76	1.59	1.67	1.75	1.68	0.37
TiO_2	3.32	3.20	3.04	3.04	3.00	2.86	2.81
P_2O_5	1.33	1.24	1.18	1.27	1.29	1.32	0.31
MnO	0.07	0.07	0.14	0.09	0.11	0.14	0.18
				Norms $(Fe^{+3}/[Fe^{+3} + Fe^{+2}]) = 0.15$			
C	0.08	–	–	–	–	–	–
OR	12.09	10.38	9.38	9.85	10.32	9.91	2.18
AB	37.83	37.92	35.89	38.17	37.84	37.67	25.83
AN	21.53	19.96	20.28	19.60	20.72	19.05	27.62
DI	–	5.22	6.02	7.40	4.03	5.84	21.24
DIWO	–	2.60	3.04	3.72	2.02	2.94	10.75
DIEN	–	1.05	1.49	1.73	0.92	1.44	5.48
DIFS	–	1.57	1.49	1.95	1.09	1.46	5.01
HY	4.49	3.61	7.01	2.79	3.18	4.74	6.66
HYEN	1.71	1.45	3.50	1.31	1.45	2.35	3.48
HYFS	2.78	2.16	3.51	1.48	1.72	2.39	3.18
FO	4.15	4.15	4.81	4.80	5.38	5.46	3.72
FA	7.44	6.82	5.31	5.97	7.03	6.11	3.75
MT	3.02	3.01	2.82	2.72	2.84	2.75	2.95
IL	6.29	6.06	5.76	5.76	5.69	5.42	5.32
AP	3.14	2.93	2.79	3.00	3.05	3.12	0.73
Total (%)	100.07	100.06	100.06	100.07	100.07	100.07	100.02

Note: Cl analysis on Sample 4-2, 110–118 cm gave <0.05 percent.

TABLE 3
Trace-Element Analyses of Lava Flows from Ōjin Seamount, DSDP Hole 430A. Concentrations in ppm

Core-Section, Interval (cm)	Flow Unit	Concentrations (ppm) Ba	Cr	Ni	Sr	Zn	Zr	Y
4-2, 110-118	1	410	<100	<2	660	148	420	57
5-1, 21-27	1	415	<100	17	670	187	400	57
5-2, 102-115	1	395	<100	18	510	141	370	40
6-1, 17-25	2	410	<100	12	690	650	430	55
6-3, 52-63	3	420	<100	13	660	178	415	52
6-4, 7-15	4	410	<100	12	650	186	435	58
6-4, 140-150	5	138	108	59	355	101	170	16

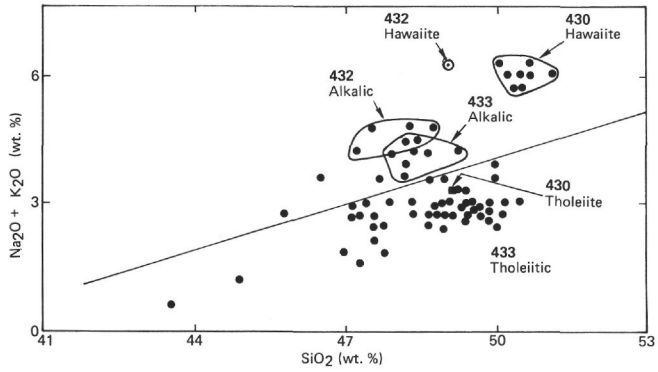

Figure 2. *Total alkalis versus silica for all Leg 55 volcanic rocks (shipboard analyses only).*

magnetic inclinations (see 430 Site Chapter), and are probably from the same eruptive event.

Petrography

Table 4 presents the modal mineralogy, the modal percentages of alteration product, the *d*-spacings of the clays, the olivine replacement, the nature and amount of vesicle filling (usually clay or zeolite), and the presence or absence of carbonate in each thin section examined. Because the modes for these samples were done using standard 30-μm-thick thin sections, the percentage of clays is probably slightly high. Figure 5 presents the modal phenocryst mineralogy versus depth in the hole.

The phenocrysts in the hawaiites, when present, are olivine and plagioclase. The groundmass minerals are olivine, clinopyroxene, plagioclase, titanomagnetite, apatite, and clay after glass. Most of the olivine is altered to saponitic clay or iddingsite, but some grains are still fresh. The textures in the hawaiites are subtrachytic, and vary from intergranular near flow margins to subophitic near flow centers. Figure 6 illustrates typical textures. Avdeiko et al. (this volume) discuss the textural variations within flows in more detail.

The phenocryst minerals in the tholeiitic basalt are olivine, augitic clinopyroxene, and plagioclase. The groundmass phases are olivine, clinopyroxene, plagioclase, titanomagnetite, ilmenite, and clays after glass. The texture is intergranular. Figure 6 illustrates the texture.

Alteration

The plagioclase, clinopyroxene, and iron-titanium oxides in both the hawaiites and the tholeiite are uniformly fresh. The interstitial glass and much of the olivine (both phenocryst and groundmass) are altered to saponitic clay. Some olivine is fresh and some altered to iddingsite.

Stratigraphy

Macdonald and Katsura (1964) and Macdonald (1968) have described a sequence of eruptive phases which commonly recur in Hawaiian volcanoes. Not each of these phases occurs at all volcanoes, but the sequence seems common enough to be considered a reference for comparison with the drilled sequences. This sequence of eruptive phases is typical of the Hawaiian chain and very rare in other oceanic islands. Macdonald (1968) identified four stages in the development of a Hawaiian volcano. They are, from earliest to latest:

1. Shield-building stage: tholeiitic basalts
2. Caldera-filling stage: tholeiitic or alkalic basalts or both. Stages 1 and 2 together make up 99 per cent of the volcano.
3. Post-caldera stage: alkalic basalts and associated differentiated lavas, about 1 per cent of the volcano.
4. Post-erosional stage: alkalic basalts, nepheline basalts, and nepheline melilite basalts, less than 1 per cent of the volcano.

In a hole drilled into a complete sequence like this it would be possible to distinguish three stages: tholeiitic basalts at the bottom, alkalic basalts and hawaiities above them, and on top a thin veneer of strongly alkalic post-erosional flows.

The drilled sequence of volcanic rocks at Site 430 is meager (about 28 m), and only one tholeiitic flow was encountered, so it is difficult to determine whether the sequence is the same as on the Hawaiian volcanoes. The Hole 430A sequence with four hawaiite flows overlying a tholeiitic flow is, however, consistent with the Hawaiian sequences. On the basis of pyroxene and feldspar chemistry (Clague et al., this volume), the hawaiites appear to belong to the caldera-filling or post-caldera stage rather than the post-erosional stage.

SITE 432

Site 432 was drilled into perched terrace deposits on the north side of Nintoku seamount at 41°20.03′N, 170°22.74′E. Hole 432A is the only hole to penetrate the volcanic sequence. Three flow units of olivine ± plagioclase ± clinopyroxene phyric alkali basalt occur in the 32 meters of basement drilled. In addition, there are cobbles of volcanic rock in a conglomerate which overlies the basalt. The one analyzed cobble is an aphanitic hawaiite.

Chemistry

Chemically the Site 432 volcanics are similar to Hawaiian-type alkalic basalts and hawaiites (Macdon-

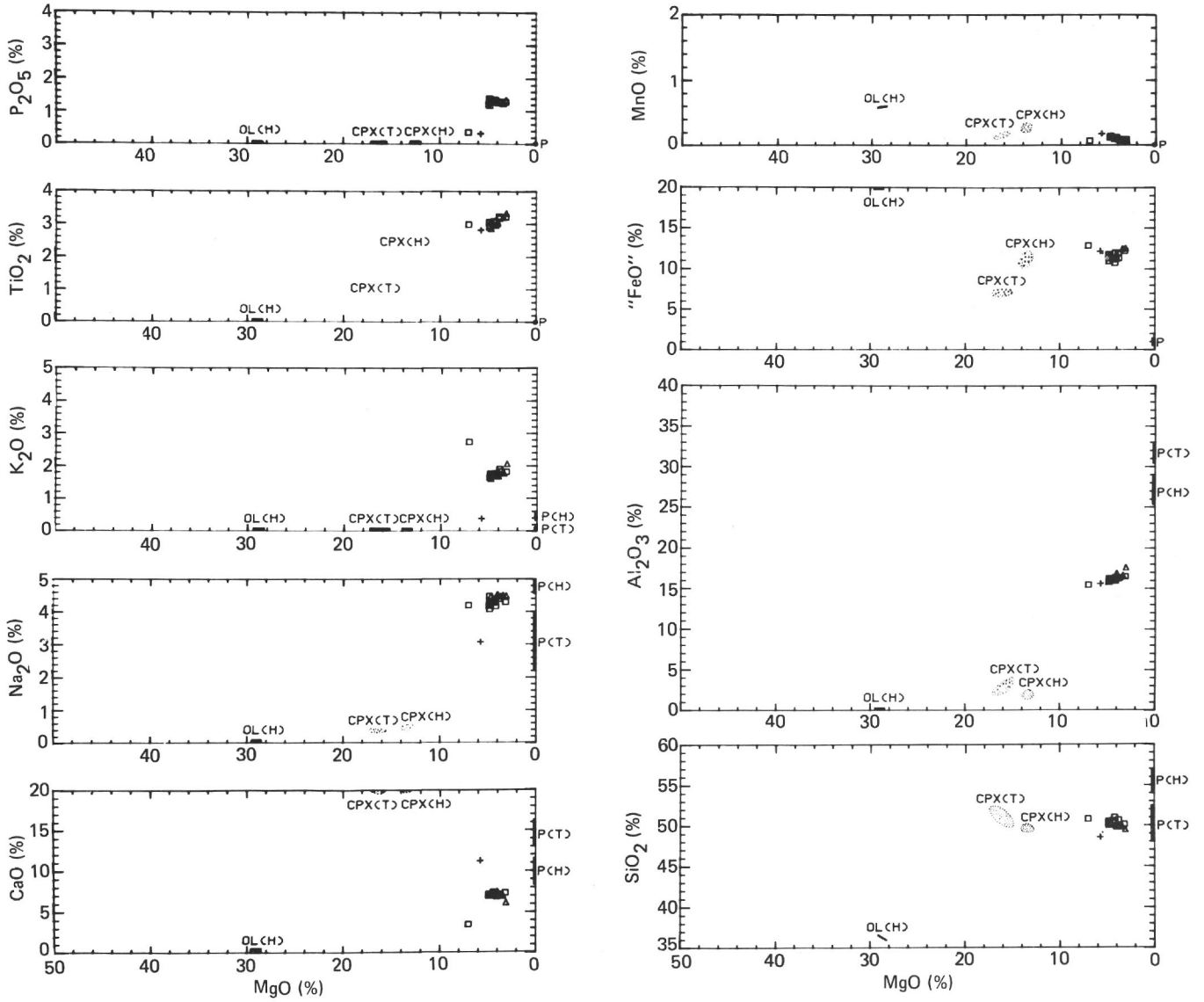

Figure 3. *MgO variation diagrams for Site 430 volcanic rocks, including phenocryst compositions (Clague et al., this volume). Point at MgO = 7.0% is sand.*

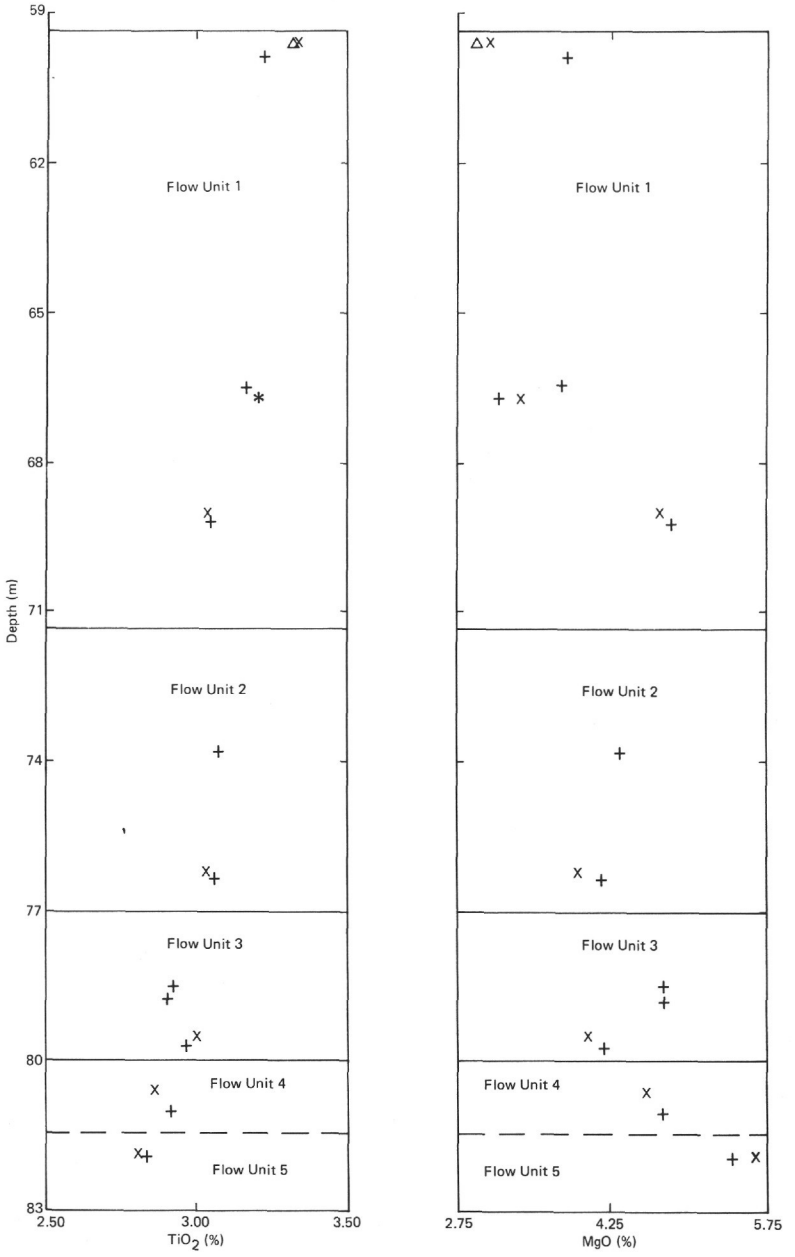

Figure 4. *Downhole variation in MgO and TiO_2 for Hole 430A volcanic rocks. + = shipboard analysis and × = shorebased analyses.*

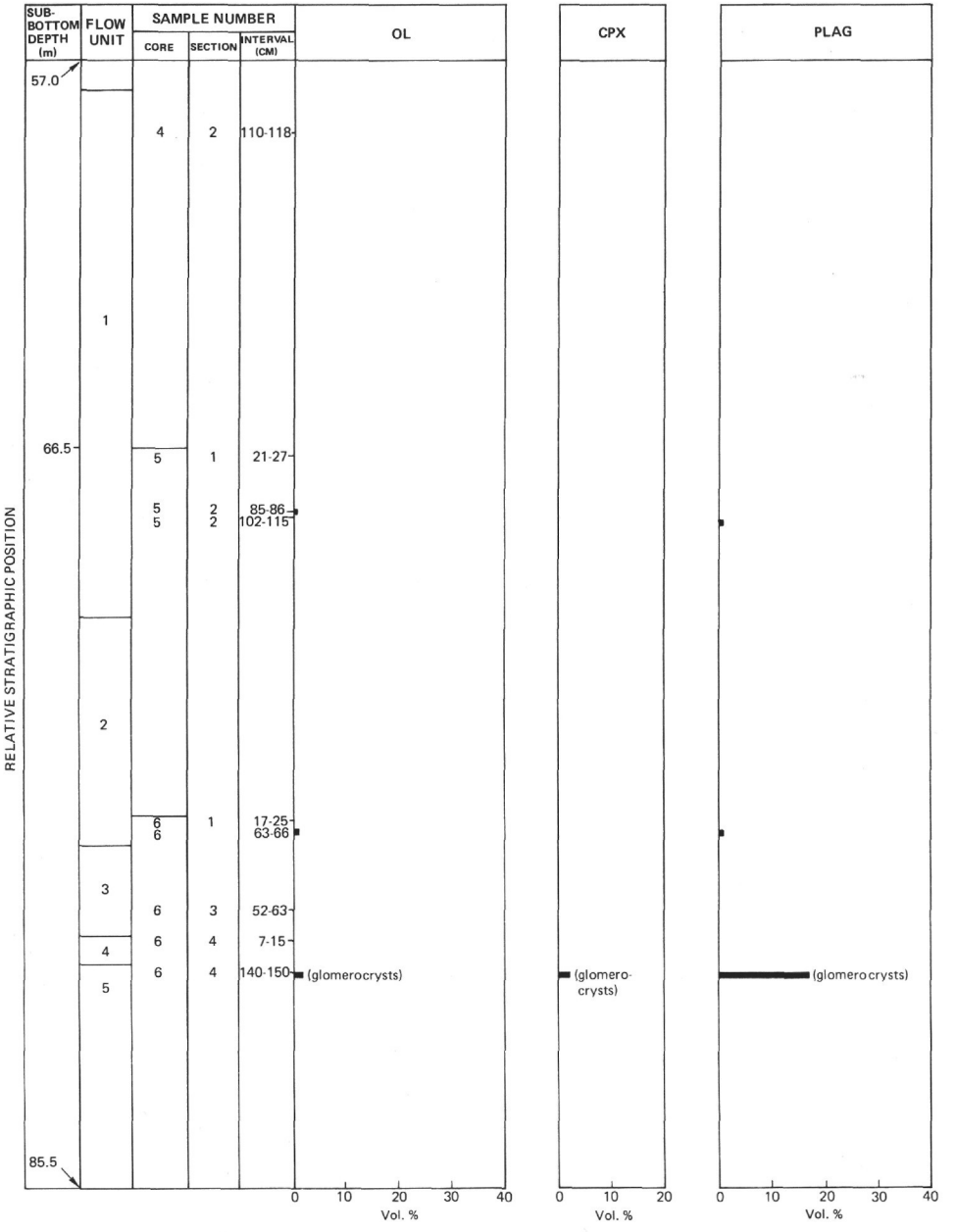

Figure 5. *Downhole variation in phenocryst mineralogy for Hole 430A volcanic rocks.*

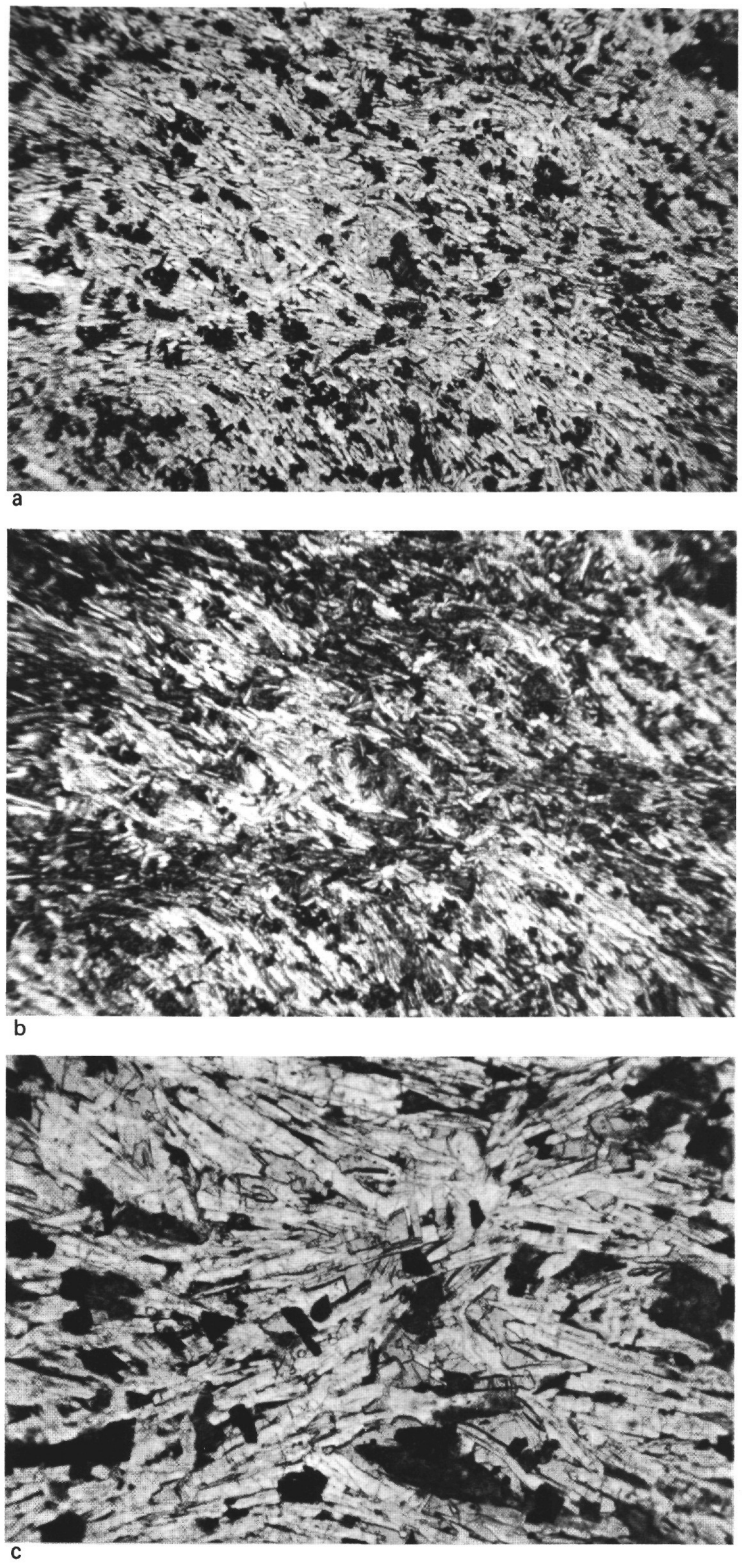

Figure 6. *Photomicrographs of Site 430 volcanic rock. A) Trachytic texture in hawaiite, Sample 430A-5-2, 120–123 cm. Plane light. Length of field is 4.9 mm. B) Same as A, but crossed nicols. Notice areas of subparallel plagioclase laths which are all in the extinction positions. C) Intergranular texture of hawaiite, Sample 430A-5-2, 120–123 cm. Notice clinopyroxene between plagioclase laths with trachytic texture. Plane light; length of field is 1.3 mm.*

TABLE 4
Petrographic Summary for Hole 430A Volcanic Rocks

			Phenocrysts & Microphenocrysts					Groundmass					
Core-Section, Interval (cm)	Flow Unit	Rock Type	Mineral	Per cent	Average Size (mm)	Per cent	Dominant Texture	Size Range (mm)	Minerals[a]	Per cent	Opaque Minerals	Alteration and Remarks[b]	Other Work
4-2, 110–118	1	Hawaiite				100	subtrachytic	0.01 –0.95 0.005–0.28 0.01 –0.40 0.005–0.40 0.01 –0.50 0.01 –0.28	pl cpx ol mt il ap	57 19 13 5 4 2	Exsolved equant timag. and elongate ilmenite. Pyrite common and chalcopyrite present in pools of clays.	22% altered, ol completely replaced by iddingsite and smectite. Smectite has basal *d*=12.62Å which splits to a 14.72Å and a 16.92Å peak after glycol. Mainly smectite A but trace of B also. Mt partly replaced by hematite.	W,X,T,M, S,K
5-1, 21–27	1	Hawaiite				99+	subtrachytic, intersertal	0.01 –1.55 0.005–0.50 0.01 –0.50 0.005–0.48 0.01 –0.65 0.01 –0.50	pl cpx ol mt il ap	62 16 7 7 4 3	Exsolved equant timag. and rare elongate ilmenite. Most timag. have undergone long-term oxidation and are flat gray to white in reflecting light.	~12% altered, ol completely replaced by smectite and rare calcite. Smectite has basal *d*=12.44Å which expands to 17.31Å after glycol. Smectite A only.	X,T,M,S, K
5-2, 85–86	1	Hawaiite	ol	<1	0.53	100	subtrachytic intersertal	0.02 –0.55 0.005–0.50 0.02 –0.50 0.02 –0.50 up to 0.50 0.005–0.008	pl cpx ol il ap mt	63 16 11 5 3 2		25% altered, nearly all ol replaced by smectite. Smectite has basal *d*=14.24Å which expands to 16.98Å after glycol. Mainly smectite A but trace of B also.	
5-2, 102–115	1	Hawaiite	pl	<1	1.35	99+	subtrachytic, intersertal	0.05 –0.60 0.04 –0.50 0.05 –0.48 0.02 –0.40 0.04 –0.49 0.05 –0.07	pl cpx ol mt il ap	60 20 10 6 2 1	Timag. and ilmenite. Timag. has ilmenite exsolution lamellae.	21% altered, nearly all ol replaced by iddingsite and smectite. Smectite has basal *d*=14.24Å which expands to 16.66Å after glycol. Mainly smectite A but trace of B also.	X,P,T,R2, M
6-1, 17–25	2	Hawaiite				100	subtrachytic	0.10 –0.70 0.05 –0.30 0.04 –0.49 0.05 –0.30 up to 0.10 0.02 –0.33	pl cpx ol mt ap il	61 23 10 5 <1 1	Equant exsolved timag. and elongate ilmenite.	~19% altered, nearly all ol replaced by iddingsite and smectite and calcite. Smectite has basal *d*= 13.80Å which expands to 17.31Å after glycol. Mainly smectite A but trace of B also.	X,P,T,R2, M
6-1, 63–66	2	Hawaiite	pl ol	<1 <1	0.83 0.55	100	subtrachytic, intersertal	0.005–0.50 0.006–0.50 0.008–0.50 0.001–0.20 0.006–0.30 0.005–0.41	pl cpx ol mt ap il	54 18 12 8 5 3		25% altered, ol completely replaced by iddingsite and smectite. Smectite has basal *d*=14.02Å which expands to 17.31Å after glycol. Mainly smectite A but trace of B also. Rims of mt altered to hematite.	
6-3, 52–63	3	Hawaiite				99+	subtrachytic	0.007–0.75 0.008–0.10 0.01 –0.09 0.03 –0.50 0.18 –0.40 0.007–0.01	pl cpx mt ol il ap	64 22 5 4 3 1	Equant exsolved timag. and elongate ilmenite.	~15% altered, ol completely replaced by smectite. Smectite has basal *d*=14.02Å which expands to 16.98Å after glycol. Mainly smectite A but trace of B also.	X,P,T,R2, M,S,K
6-4, 7–15	4	Hawaiite				100	subtrachytic	0.01 –0.90 0.006–0.20 0.01 –0.64 0.004–0.20 0.005–0.30 up to 0.08	pl cpx ol mt il ap	63 17 12 4 4 <1	Timag and ilmenite.	28% altered, 85% of ol replaced by iddingsite and smectite. Smectite has basal *d*=13.80Å which expands to 17.31Å after glycol. Both smectite A and B are abundant. Mt partly replaced.	X,T,M,S, K
6-4, 140–150	5	Plagioclase Tholeiite	pl cpx ol	17 2 1	1.47 1.33 1.22	87	Glomerophyric intergranular	0.25 –0.50 0.006–0.40 0.005–0.08 0.008–0.10 0.01 –0.50	pl cpx mt il ol	42 32 2 2 2	Timag. and ilmenite. Pyrite is rare.	5% altered, ol completely replaced by iddingsite and smectite. Smectite has basal *d*=15.49Å that expands to 17.31Å after glycol. Only smectite A is present. Pl phenocrysts are strongly zoned and contain glass inclusions.	X,P,T,R2, M,S,K

Note: pl = plagioclase; ol = olivine; cpx = clinopyroxene; il = ilmenite; mt = magnetite; ap = apatite; kf = potash feldspar.
[a]By modal analysis of ordinary thin sections. Magnetite distinguished from ilmenite by shape. All percentages corrected for low-temperature alteration.
[b]Smectite A is expandable on glycolation. Smectite B is only partially expandable on glycolation. Chlorite is not expandable.
Other Work: W = wet chemical analysis.
X = X-ray fluorescence for majors
P = microprobe for majors (Bence et al.)
T = X-ray fluorescence for trace elements
R1 = INAA for rare earths and trace elements (Clague and Frey)
R2 = ES for rare earths and trace elements (Bence et al.)
S = Sr isotopic analysis (Lanphere et al.)
K = K-Ar ages (Dalrymple et al.)
M = microprobe mineral analyses (Clague et al.)

ald, 1968). Table 5 presents the post-cruise major-element data both as received and dry-reduced, along with CIPW norms assuming $Fe^{+3}/Fe^{+3} + Fe^{+2} = 0.15$. Table 6 presents the post-cruise trace-element data. Figure 2 plots total alkalis versus silica. Figure 7 presents MgO variation diagrams and Figure 8 shows composition versus depth, using both the shore-based and shipboard analyses.

TABLE 5
Chemical Analyses and Norms of Volcanic Rocks from Hole 432A, Nintoku Seamount

Core-Sec., Interval (cm)	2-1, 86–96	2-3, 37–43	3-2, 120–126	5-2, 57–66
Flow Unit	1	1	2	3
	As Received			
SiO_2	46.38	46.27	46.33	46.34
Al_2O_3	16.05	17.70	16.03	16.07
Fe_2O_3	5.63	10.00	4.74	4.71
FeO	5.82	2.10	8.64	8.45
MgO	5.38	3.52	5.72	5.84
CaO	8.71	9.54	8.20	8.16
Na_2O	3.54	3.52	2.68	3.56
K_2O	1.14	1.41	1.09	1.04
H_2O^+	1.76	1.47	1.30	1.60
H_2O^-	1.89	1.87	0.66	0.98
TiO_2	2.54	2.46	2.94	2.90
P_2O_5	0.80	0.52	0.49	0.48
MnO	0.14	0.09	0.18	0.18
CO_2	0.22	0.13	0.02	0.05
Total (%)	100.00	100.60	100.02	100.36
	Dry Reduced Normalized			
SiO_2	48.53	48.13	47.49	47.65
Al_2O_3	16.79	18.41	16.43	16.52
FeO	11.39	11.55	13.23	13.05
MgO	5.63	3.66	5.86	6.00
CaO	9.11	9.92	8.40	8.39
Na_2O	3.70	3.66	3.77	3.66
K_2O	1.19	1.47	1.12	1.07
TiO_2	2.66	2.56	3.01	2.98
P_2O_5	0.84	0.54	0.50	0.49
MnO	0.15	0.09	0.18	0.19
	Norms $(Fe^{+3}/[Fe^{+3}+Fe^{+2}]) = 0.15$			
OR	7.02	8.67	6.60	6.31
AB	30.96	25.88	28.73	29.61
AN	25.64	29.41	24.55	25.43
NE	0.16	2.73	1.68	0.70
DI	11.52	13.54	11.39	10.66
DIWO	5.84	6.76	5.75	5.39
DIEN	3.05	2.87	2.86	2.72
DIFS	2.63	3.90	2.78	2.55
FO	7.67	4.36	8.20	8.54
FA	7.29	6.53	8.79	8.82
MT	2.75	2.79	3.20	3.15
IL	5.04	4.85	5.70	5.65
AP	1.97	1.28	1.18	1.16
Total (%)	100.04	100.03	100.03	100.03

TABLE 6
Trace-Element Analyses of Lava Flows from Nintoku Seamount, DSDP Hole 432A

Core-Section, Interval (cm)	Flow Unit	Concentrations (ppm) Ba	Cr	Ni	Sr	Zn	Zr	Y
2-1, 86–96	1	365	<100	45	640	123	265	36
2-3, 37–43	2	375	111	79	640	103	169	12
3-2, 120–126	3	365	113	49	420	99	184	<9
5-2, 57–66	3	400	110	47	495	126	191	33

The three alkali basalt flows at Site 432 are generally similar to each other. Flows 1 and 2 have similar magnetic inclinations (−66° to −67°); Flow Unit 3 has a much lower inclination (−29°). Although no quantitative calculations have been made, Flows 1 and 2 may be related. Because of the large difference in magnetic inclination, Flow Unit 3 is probably not directly related to the others. Flow Unit 1 appears to be somewhat more differentiated than Flow Unit 2. If they are related, it is not by olivine fractionation alone. The composition of the hawaiite cobble is considerably different from the alkali basalts. Because of the small number of analyzed flows it is not possible to usefully examine the chemical relationships between the two rock types.

Petrography

Table 7 presents the modal mineralogy, the modal percentages of alteration product, the *d*-spacings of the clay minerals, the olivine replacement, the nature and amount of vesicle filling (usually clay or zeolite), and the presence or absence of carbonate in each Site 432 thin section examined. Figure 9 presents the modal phenocryst mineralogy versus depth for the samples examined.

All three alkali basalt flows contain plagioclase, clinopyroxene, and olivine phenocrysts. Flow Units 1 and 2 are richer in plagioclase: Flow 3 is richer in clinopyroxene. The groundmass minerals are olivine, clinopyroxene, plagioclase, titanomagnetite, apatite, clay after glass, and a trace of biotite. The hawaiite cobble is essentially aphyric. Its groundmass minerals are olivine, clinopyroxene, plagioclase, titanomagnetite, apatite, and clay after glass.

The textures in the alkali basalts range from intersertal through intergranular to sub-ophitic or ophitic. The hawaiite is subtrachytic and intergranular. Figure 10 presents photomicrographs of typical textures in these rocks.

Alteration

The plagioclase and clinopyroxene in both the alkali basalts and the hawiite are uniformly fresh. The interstitial groundmass glass and much of the olivine are altered to saponitic clay. Some of the olivine is fresh and some altered to iddingsite. Much of the titanomagnetite contains exsolved ilmenite, and some is altered to titanomaghemite.

Stratigraphy

As at Site 430, because of technical problems, the drilling at Site 432 did not continue deep enough to determine whether the sequence of flows is the same as the typical Hawaiian sequence. The presence of alkali basalts at the top, however, is consistent with this sequence. On the basis of their pyroxene and feldspar chemistry, the alkali basalt flows appear to belong to the caldera-filling stage or post-cladera stage, and not to the post-erosional stage (Clague et al., this volume).

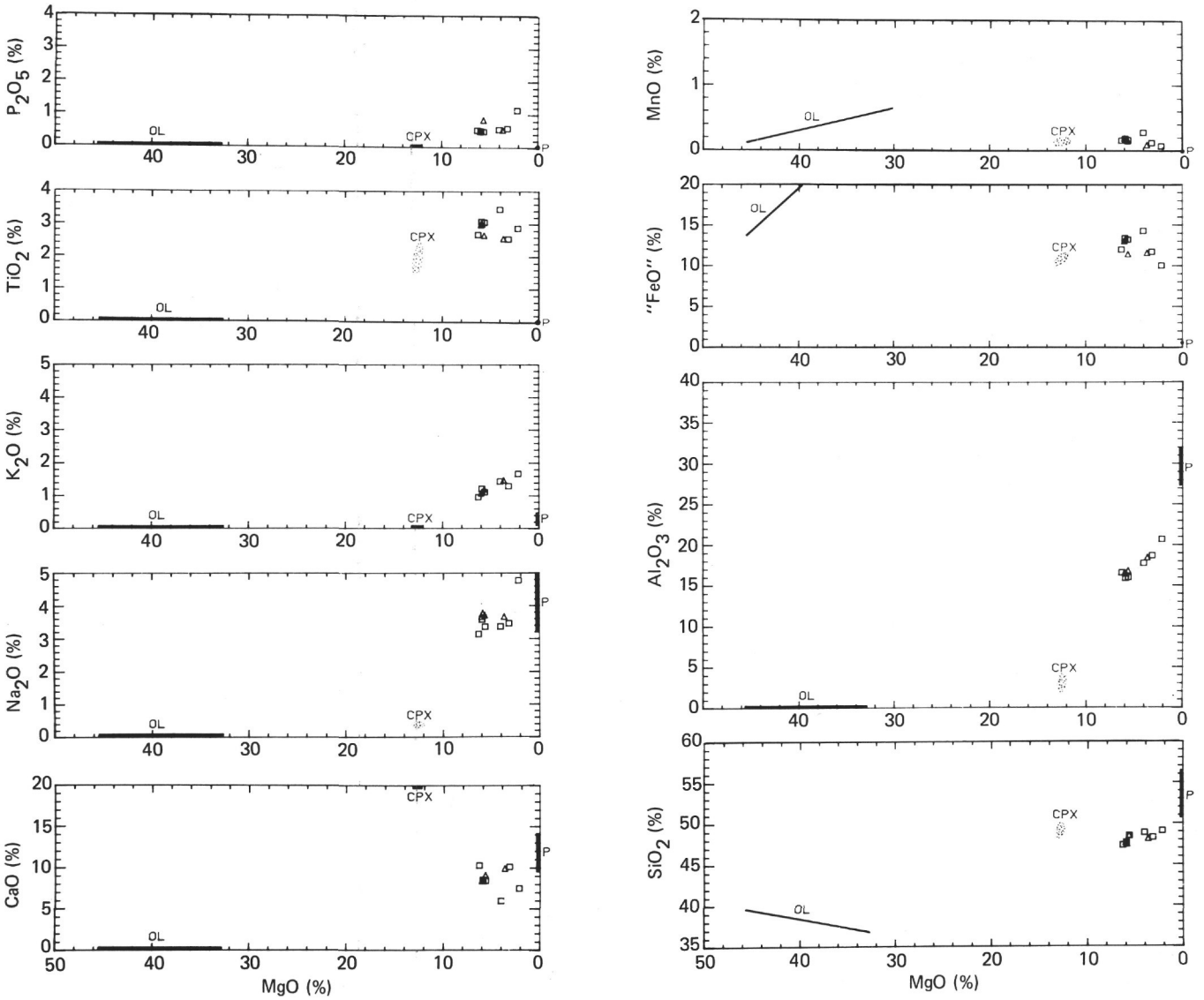

Figure 7. *MgO variation diagrams for Site 432 volcanic rocks, including phenocryst compositions (Clague et al., this volume).*

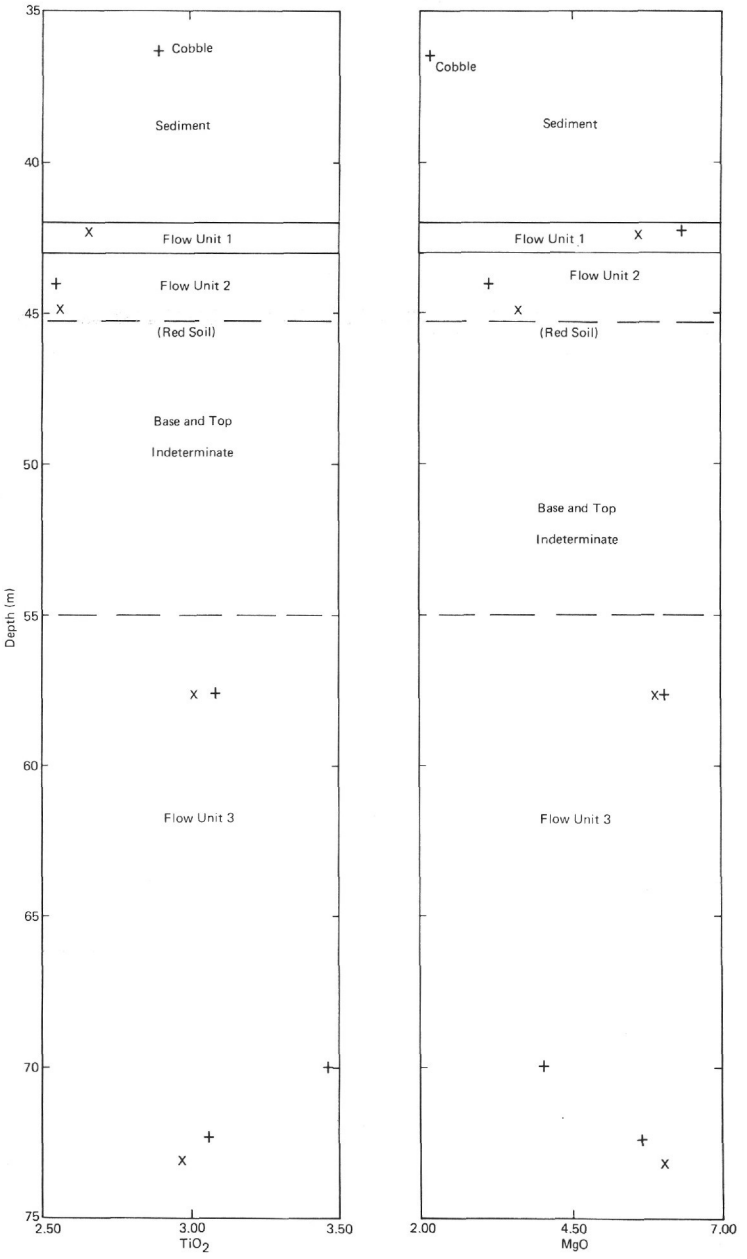

Figure 8. *Downhole variation in MgO and TiO_2 for Hole 432A volcanic rocks. + = shipboard analysis and × = shorebased analysis.*

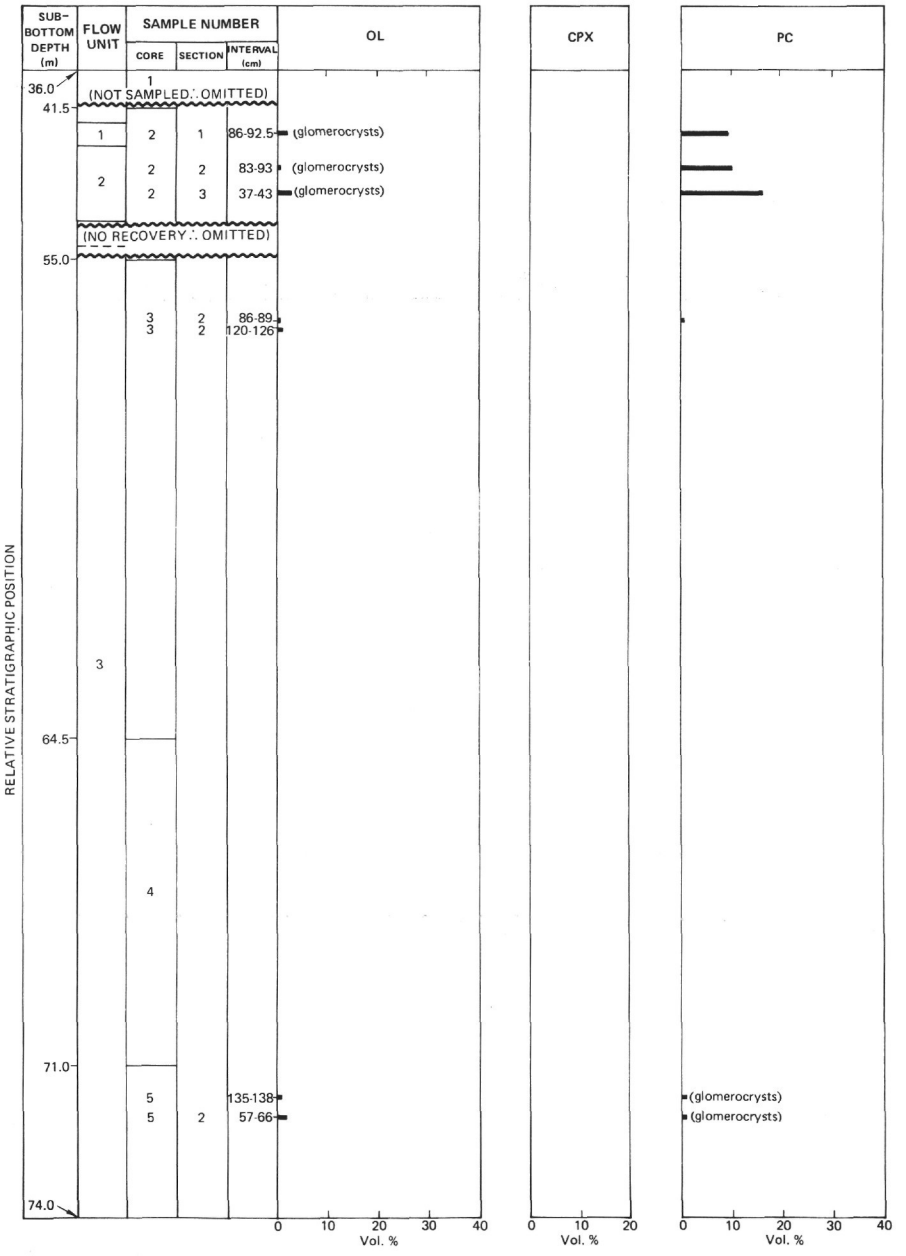

Figure 9. *Downhole variation in phenocryst mineralogy for Hole 432A volcanic rocks.*

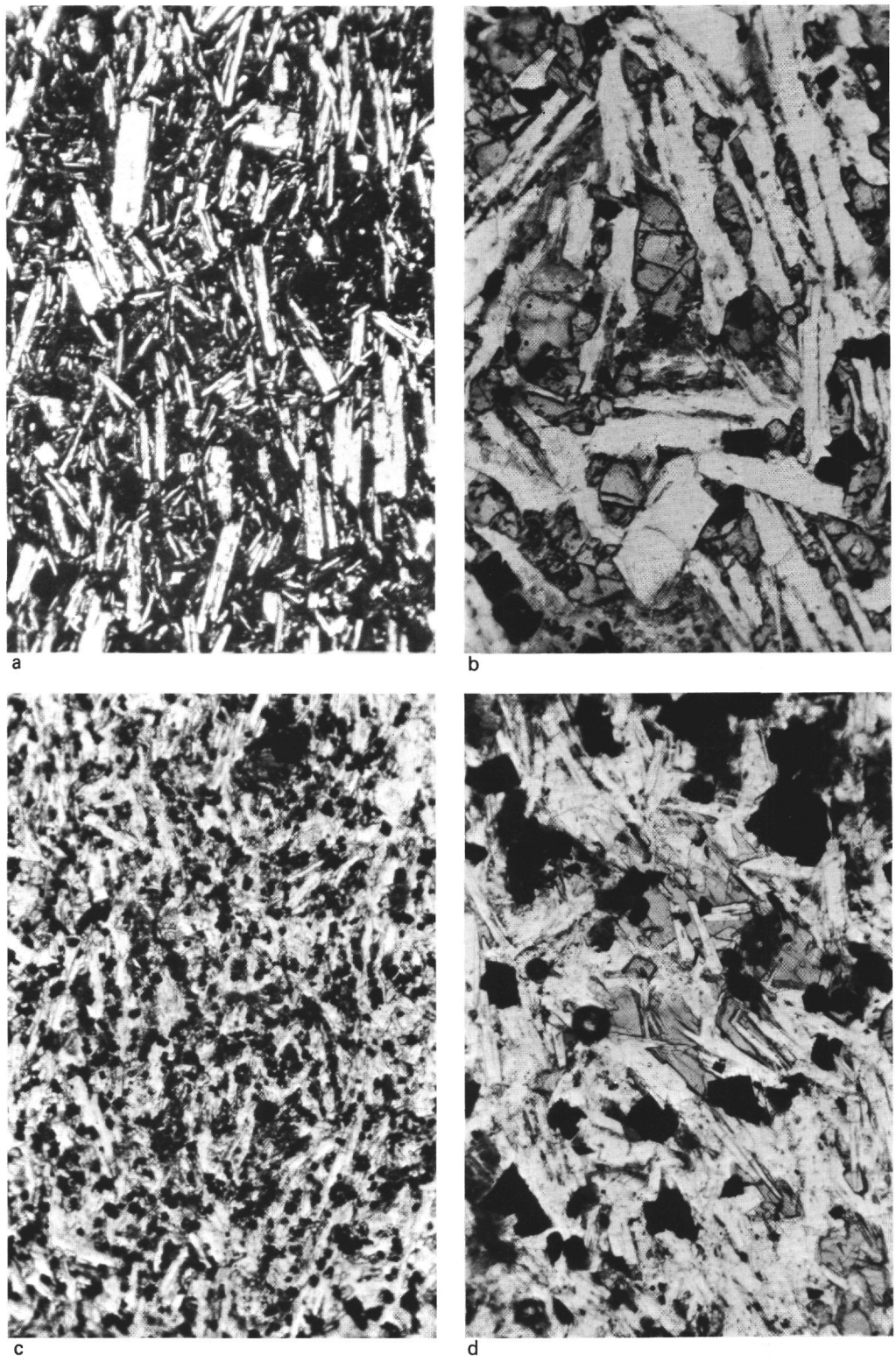

Figure 10. *Photomicrographs of Site 432 volcanic rocks. A) Trachytic texture of hawaiite cobble, Sample 432A-1-1, 30–40 cm, in carbonate-cemented conglomerate overlying the volcanic sequence. Note serrate grain-size distribution. Crossed nicols. Length of field is 1.3 mm. B) Intergranular texture in center of alkalic basalt flow, Sample 432A-2-1, 83–85 cm. Plate light. Length of field is 1.3 mm. C) Fine-grained intergranular texture from near top of alkalic basalt flow, Sample 432A-3-2, 106–108 cm. Plane light. Length of field is 1.3 mm. D) Ophitic texture from center of alkalic basalt flow, Sample 432A-5-2, 55–58 cm. Plane light. Length of field is 1.3 mm.*

TABLE 7
Petrographic Summary for Hole 432A Basalts

			Phenocrysts & Microphenocrysts			Vesicles				Groundmass
Core-Section, Interval (cm)	Flow Unit	Rock Type	Mineral	Per cent	Average Size (mm)	Per cent	Size Range (mm)	Average Size (mm)	Shape	Per cent
2-1, 86–92.5	1	Alkalic Basalt	pl ol	9 2	2.48 0.54					89
2-2, 83–93	2	Alkalic Basalt	pl ol	10 <1	1.37 1.00	6	0.10–1.11	0.63	irregular-elongated in direction of flow	90
2-3, 37–43	2	Alkalic Basalt	pl ol	16 3	2.63 0.67	5	0.19–0.90	0.51	rounded	81
3-2, 86–89	3	Alkalic Basalt	pl ol	<1 <1	1.40 0.50					99+
3-2, 120–126	3	Alkalic Basalt	ol	1	1.40					99
5-1, 135–138	4	Alkalic Basalt	ol pl	1 1	0.84 0.73					98+
5-2, 57–66	4	Alkalic Basalt	pl ol	<1 2	 0.55					97+

Note: pl = plagioclase; ol = olivine; cpx = clinopyroxene; il = ilmenite; mt = magnetite; ap = apatite; kf = potash feldspar.

[a]By modal analysis of ordinary thin sections. Magnetite distinguished from ilmenite by shape. All percentages corrected for low-temperature alteration.

[b]Smectite A is expandable on glycolation. Smectite B is only partially expandable on glycolation. Chlorite is not expandable.

Other Work: W = wet chemical analysis
X = X-ray fluorescence for majors
P = microprobe for majors (Bence et al.)
T = X-ray fluorescence for trace elements
R1 = INAA for rare earths and trace elements (Clague and Frey)
R2 = ES for rare earths and trace elements (Bence et al.)
S = Sr isotopic analysis (Lanphere et al.)
K = K–Ar ages (Dalrymple et al.)
M = microprobe mineral analyses (Clague et al.)

TABLE 7 – *Continued*

Dominant Texture	Size Range (mm)	Groundmass Minerals[a]	Per cent	Opaque Minerals	Alteration and Remarks[b]	Other Work
sub-ophitic	0.10 –2.30 0.02 –0.50 0.005–0.10 0.06 –0.42 0.05 –0.20 0.01 –0.19	pl cpx mt ol ap il	52 25 6 4 1 1	Equant timag. rare pyrite	25% altered, ol completely replaced by iddingsite and smectite. Smectite has basal d=14.24Å which expands to 17.31Å after glycol. Both smectite A and B are abundant. Mt partly replaced by hematite.	X,P,T,R2,M
subtrachytic glomerophyric	0.05 –5.00 0.10 –0.67 0.05 –0.50 0.01 –0.10 0.05 –0.10 0.02 –0.21	pl cpx ol mt ap il	52 19 8 8 1 1		16% altered, ol completely replaced by iddingsite. Smectite has basal d= 13.38Å which expands to 16.98Å after glycol. Only a minor amount of smectite A is present. Some mt partly replaced by hematite. Vesicles have botryoidal clay linings.	
microlitic intergranular	0.02 –3.30 0.03 –0.50 0.05 –0.50 0.01 –0.10 0.01 –0.30 0.03 –0.25	pl cpx ol mt ap il	49 21 4 4 2 1	Equant timag.	12% altered, ol completely replaced by iddingsite, smectite and calcite. Smectite has basal d=16.98Å after glycol. Only a minor amount of smectite A is present. Vesicles generally filled with yellow smectite.	X,P,T,R2,S, K,M
intergranular	0.05 –0.41 0.01 –0.10 (0.01)[2] 0.01 –0.42	pl cpx mt ol	53 29 11 6		5% altered, ol is 80–85% replaced by olive green smectite. Smectite has basal d=14.48Å which splits to form 2 peaks, d=14.48Å (chlorite?) and d=17.31Å. Only chlorite(?) and smectite B are present.	
microlitic, intergranular	0.02 –0.50 0.008–0.10 0.002–0.20 0.05 –0.50 0.01 –0.10	pl cpx mt ol il	58 28 10 1 2	Equant timag. Both pyrite and chalcopyrite are present.	~2% altered, ol is 40% replaced by olive green smectite. Smectite has basal d=14.48Å that expands to 17.31Å after glycol. Only smectite B and chlorite (?) are present. Rare phillipsite in groundmass.	X,P,T,R2,S, K,M
subtrachytic, ophitic	0.02 –0.73 0.01 –0.10 0.05 –0.50 0.005–0.40 0.005–0.40 0.01 –0.40	pl cpx ol mt il ap	54 23 11 7 2 2		24% altered, ol is 80–85% replaced by olive green smectite. Smectite has basal d=14.48Å that expands to 17.31Å after glycol. Only smectite B and chlorite(?) are present.	
subtrachytic, ophitic	0.05 –0.71 0.01 –0.25 0.01 –0.50 0.005–0.25 0.01 –0.20	pl cpx ol mt il	52 24 13 4 4	Timag. Ilmenite may be present as very tiny elongate crystals. Pyrite is present and the olivine phenocrysts contain rare chromite.	13% altered, ol is 90% replaced by olive green smectite. Smectite has basal d=14.48Å that expands to 17.31Å after glycol. Only smectite B and chlorite(?) are present.	X,T,M,S,K

SITE 433

Site 433 was drilled into a lagoonal sediment pond on the northwest side of Suiko seamount at 44° 46.63′N, 170° 01.23′E. It is the major site of Leg 55, and the material available for study is far more extensive than for Site 430 and 432. Three holes — 433A, 433B, and 433C — reached volcanic basement and 433C penetrated about 387 meters of volcanic material. This is the longest section to be studied in detail in the entire Hawaiian-Emperor chain. As discussed in the Site Chapter for Site 433 (Leg 55 Scientific Staff, this volume), there are 67 numbered volcanic units in Hole 433C, and probably 114 individual lava flows. All are subaerial. Most of these that are reasonably fresh have been analyzed either on board the *Challenger* or after the cruise.

Chemistry and Classification

The rocks recovered at Site 433 are all alkalic basalts, tholeiitic basalts, or tholeiitic picrites. Table 8 presents

the post-cruise major-element analyses both as received and dry-reduced, along with CIPW norms assuming $Fe^{+3}/Fe^{+3} + Fe^{+2} = 0.15$. Table 9 presents the post-cruise trace-element data. In general, these data are for the least-altered samples available, and are usually from relatively massive flow interiors. Figure 2 presents the total alkalis versus silica data, Figure 11 gives MgO variation diagrams, and Figure 12 shows the chemical variation with depth in the hole for the Site 433 volcanic rocks.

The top three flow units (1 through 3) are alkali basalts (Figure 2) that are very similar. They also have similar magnetic inclinations, and may well be genetically related.

We have classified the rest of the flows as tholeiitic picrites (oceanites) or tholeiitic basalts. Most of these fall well within the tholeiitic field on the plot of total alkalis versus silica. Those that fall on the alkali side of the dividing line usually have very high K_2O contents. The X-ray diffraction work (appendix, following this chapter) indicates that at least some of these samples contain phillipsite. Their apparent alkali nature, then, is a result of secondary alteration. Rare-earth-element patterns (Clague and Frey, this volume) and pyroxene chemistry (Clague et al., this volume) indicate that all the flows examined below Flow Unit 3 are best classified as tholeiitic.

Petrography

The appendix following this chapter presents the modal mineralogy, the modal percentage of alteration minerals, the *d*-spacings of the clays, the olivine replacement, the nature and amount of vesicle filling (usually clay and zeolite), and the presence or absence of carbonate in each Site 433 thin section examined. Figure 13 presents the modal phenocryst mineralogy versus depth for the samples examined.

The three alkalic flows contain olivine, clinopyroxene, and plagioclase phenocrysts in varying but approximately equal proportions.

The groundmass minerals in the alkalic flows are olivine, clinopyroxene, plagioclase, titanomagnetite, apatite, and clay after glass. Most of the olivine is altered to clay or iddingsite, although some is fresh. The textures in the alkalic basalts are subtrachytic, and vary from intergranular near flow margins to sub-ophitic in flow centers. Figure 14 illustrates the textural variation.

The tholeiitic basalts and picrites usually have only olivine phenocrysts or olivine, clinopyroxene, and plagioclase phenocrysts. A few are essentially aphyric or have only olivine and plagioclase, olivine and clinopyroxene, or clinopyroxene and plagioclase. The groundmass minerals invariably include olivine, clinopyroxene, plagioclase, titanomagnetite, ilmenite, sulfide blebs, and clay after glass. Only a few (Samples 433C-24-7, 133-139 cm, 37-3, 79-87 cm, and 39-5, 87-94 cm) contain, in addition, groundmass or microphenocryst pigeonite. The textures in the tholeiites vary from interstitial to intergranular to sub-ophitic. The flow tops and bottom must originally have been nearly all glass. Figure 14 illustrates typical textures.

Alteration

The Site 433 basalts vary from almost fresh (only interstitial glass altered to clay) to extensively altered. The alkalic basalts are less altered than the tholeiites. As at Sites 430 and 432, the plagioclase and clinopyroxene are usually unaltered. The titanomagnetite, expecially in the tholeiites, has usually undergone oxidation exsolution of ilmenite. The groundmass glass and most of the olivine is altered to saponitic clay. Some of the olivine is fresh and some has altered to iddingsite.

Stratigraphy

Hole 433C is the only hole drilled on Leg 55 which penetrated deep enough to compare the sequence of lava types with the standard Hawaiian sequence, and it appears that the Hole 433C sequence is similar to many exposed Hawaiian sequences. The top few flows are alkalic basalts and the lower bulk of the volcano is tholeiitic. Pyroxene and feldspar chemistry (Clague et al., this volume) indicates that the alkalic basalts belong to the caldera-filling stage or post-caldera stage and not the post-erosional stage. No flows in any of the Leg 55 holes have been identified as post-erosional.

Within the tholeiitic sequence the flows can be divided into 25 stratigraphically, chemically, and mineralogically coherent groups consisting of from one to six flows. Chemically these groups can best be distinguished on plots of Zr, a magmatophile element, versus Ni, which preferentially enters olivine (Figure 15). They can also be distinguished on plots of TiO_2 versus MgO (Figures 16 and 17). Table 10 lists the groups, along with their flow units, depths and core intervals, phenocryst mineralogy, chemical type, and the magnetic units (see 433 Site Report, this volume). Figure 12 illustrates the positions of the groups on plots of TiO_2 and MgO versus depth.

The Ni and MgO variation diagrams indicate that there are two kinds of tholeiitic basalt: those with relatively high TiO_2/MgO and Zr/Ni (high-Zr type) and those with relatively low TiO_2/MgO and Zr/Ni (low-Zr type). These two types correspond to the high-and low-La/MgO types of Clague and Frey (this volume). The two types are interbedded throughout the section, sometimes flow by flow, sometimes in longer sequences.

The low-Zr type is more abundant, and includes both olivine phyric basalts and picrites and more differentiated olivine, clinopyroxene, and plagioclase phyric basalts. Clinopyroxene and plagioclase phenocrysts first appear in any abundance at about 8 per cent MgO.

The high-Zr type is dominated by olivine phyric basalts and picrites. Only three flows (27, 35, and 64) contain olivine, clinopyroxene, and plagioclase phenocrysts, and one (19a) contains olivine and clinopyroxene. MgO content in Flow Unit 35 is 10.44 per cent; in the other multiply saturated flows it is less. Phenocryst clinopyroxene and plagioclase free flows occur to MgO values as low as 8.8 per cent. It does appear, though, that clinopyroxene and plagioclase phenocrysts occur at

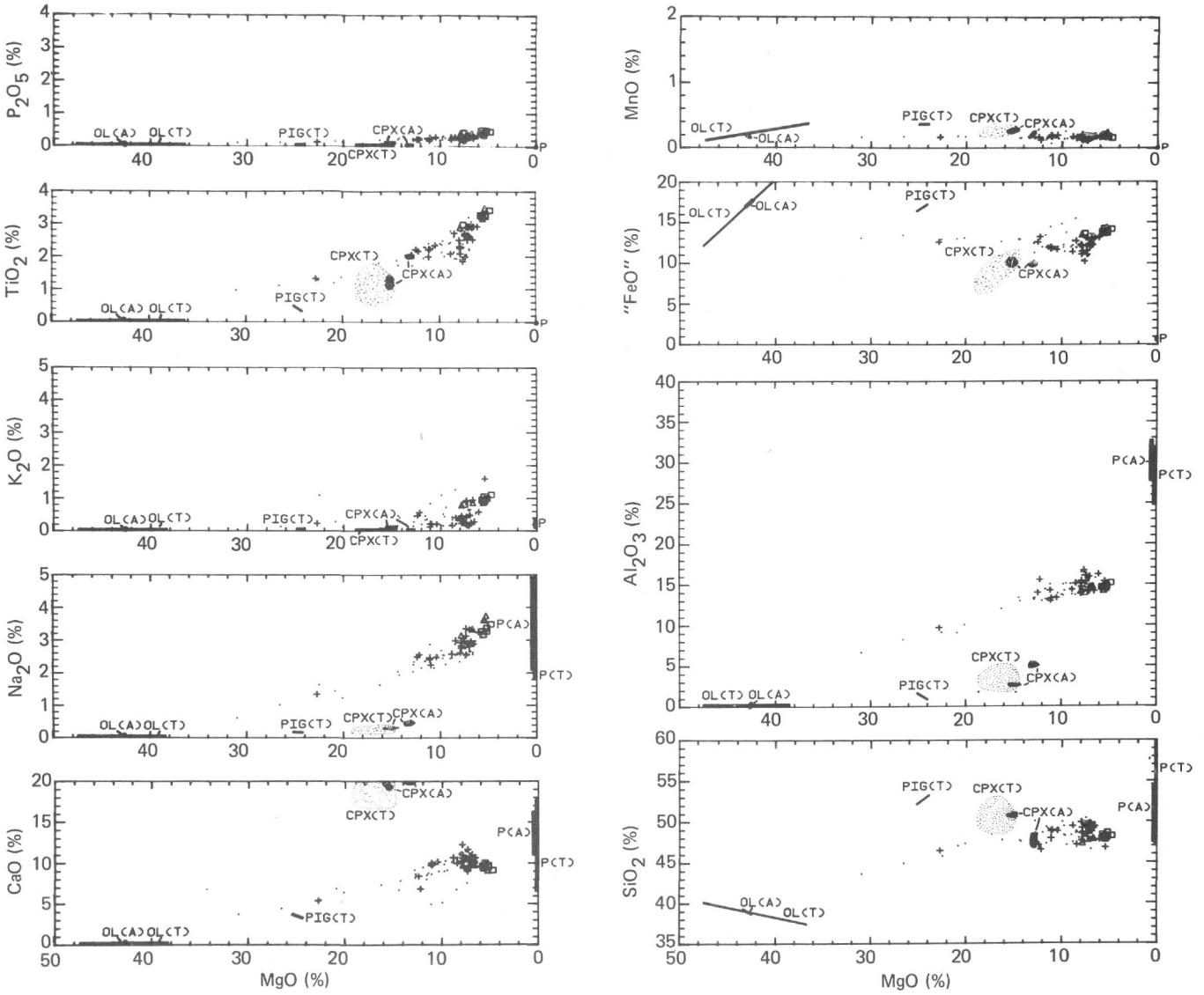

Figure 11. *MgO variation diagrams for Site 433 volcanic rocks, including phenocryst compositions (Clague et al., this volume).*

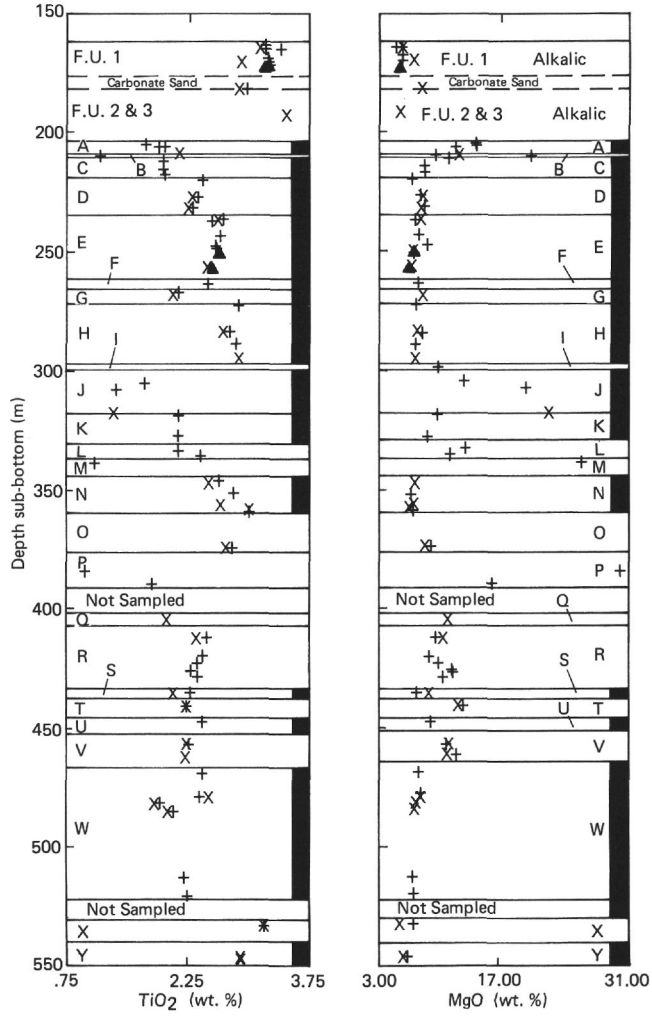

Figure 12. *Stratigraphy and chemical variation of TiO_2 and MgO within the Hole 433C volcanic sequence. Stratigraphic units correspond to those in Figures 15 and 16. Blackband indicates low-Zr tholeiite type, white band indicates high-Zr type; except for the three alkalic flows at the top. + = shipboard analysis, and × = shorebased analysis.*

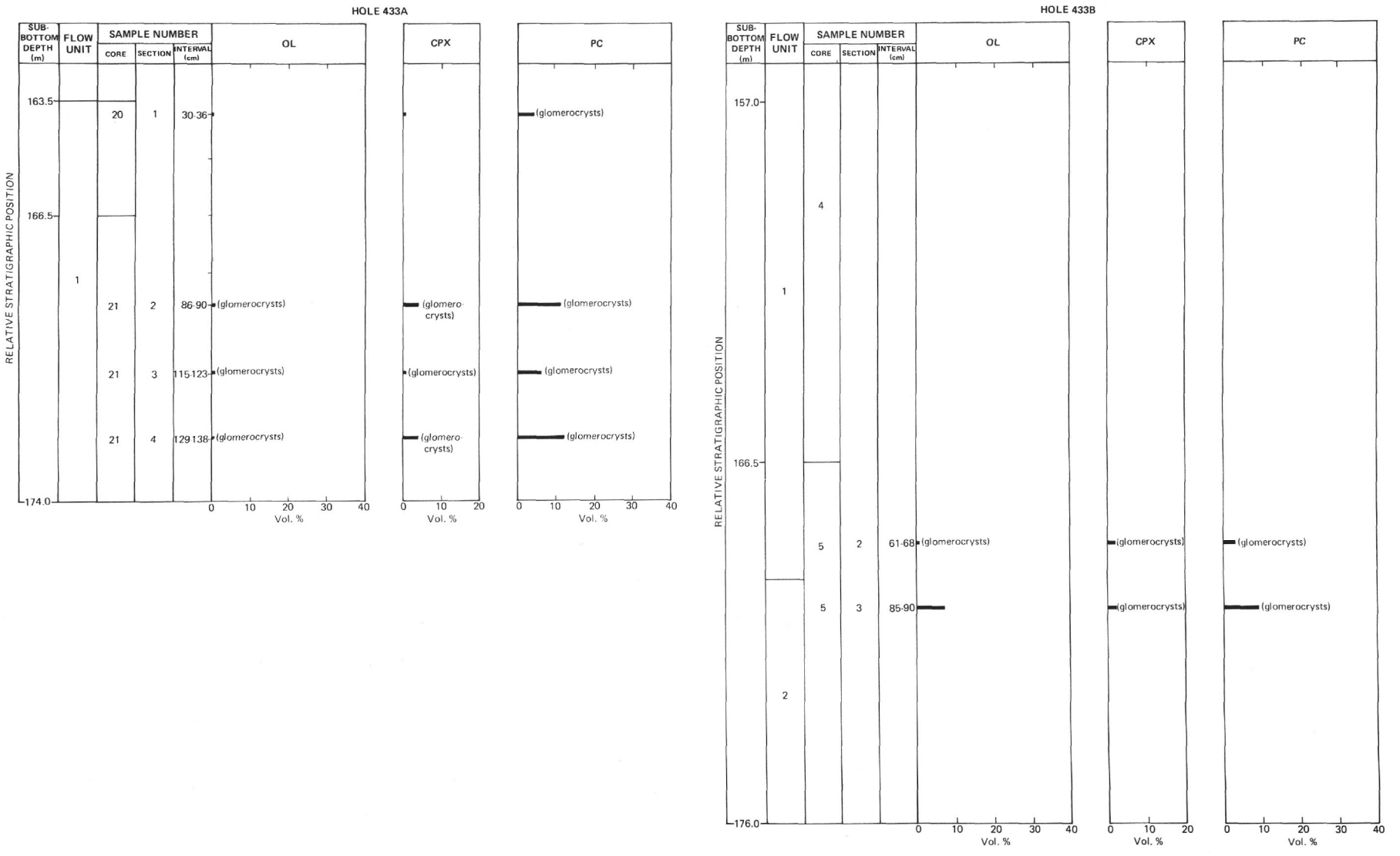

Figure 13. *Downhole variation in phenocryst mineralogy for Hole 433A volcanic rocks from Hole (a) 433A, (b) 433B, and (c) 433C.*

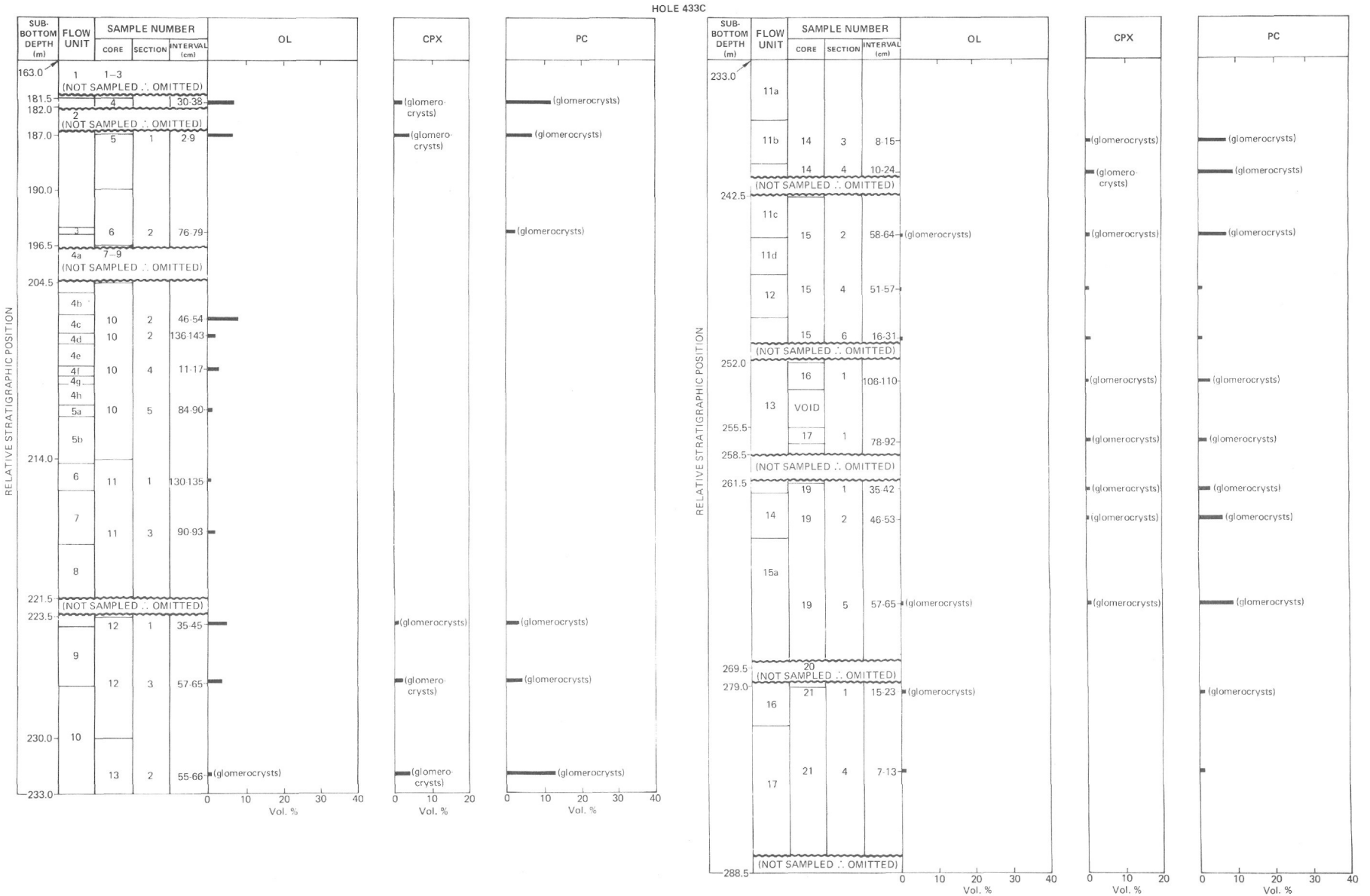

Figure 13. *(Continued).*

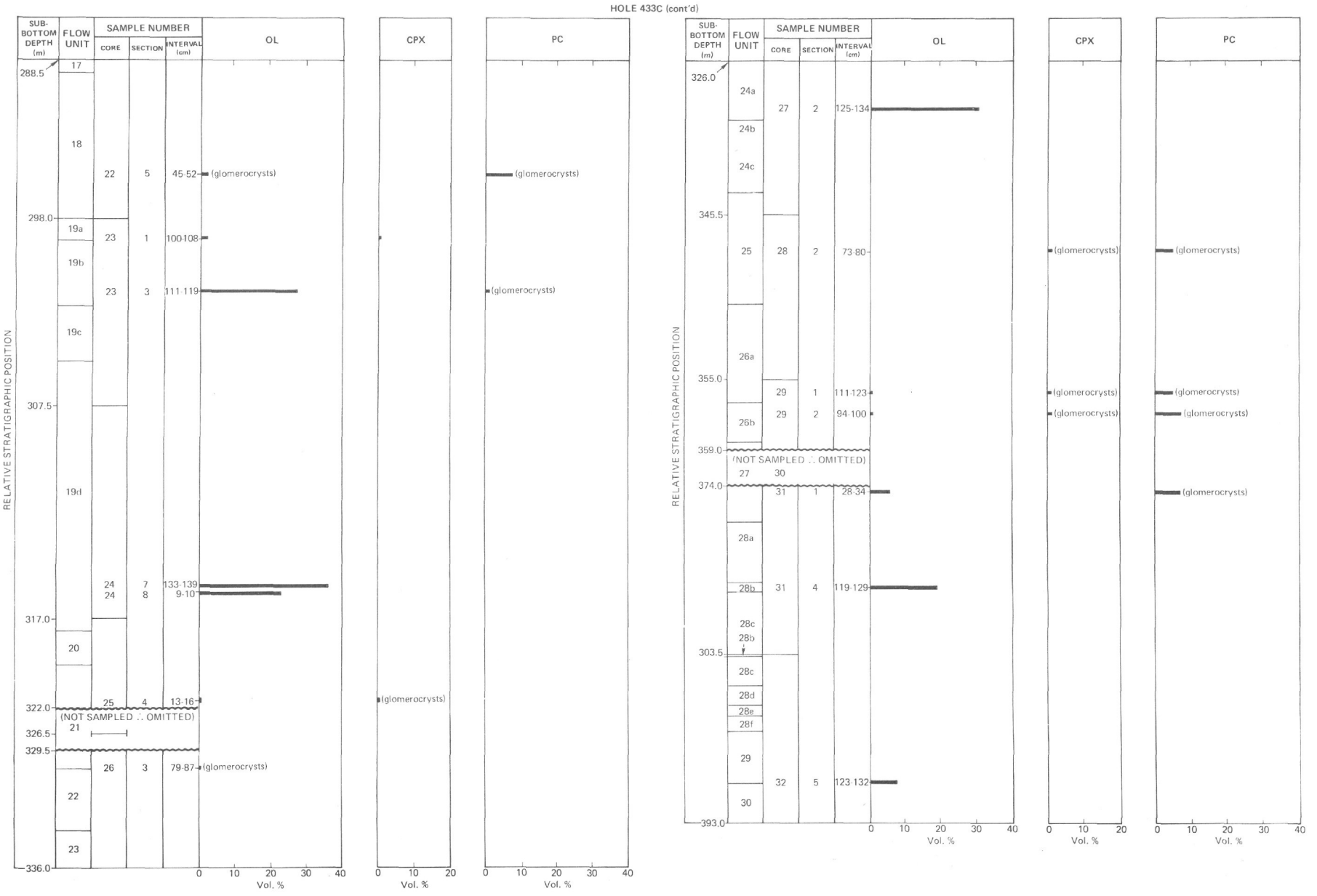

Figure 13. *(Continued).*

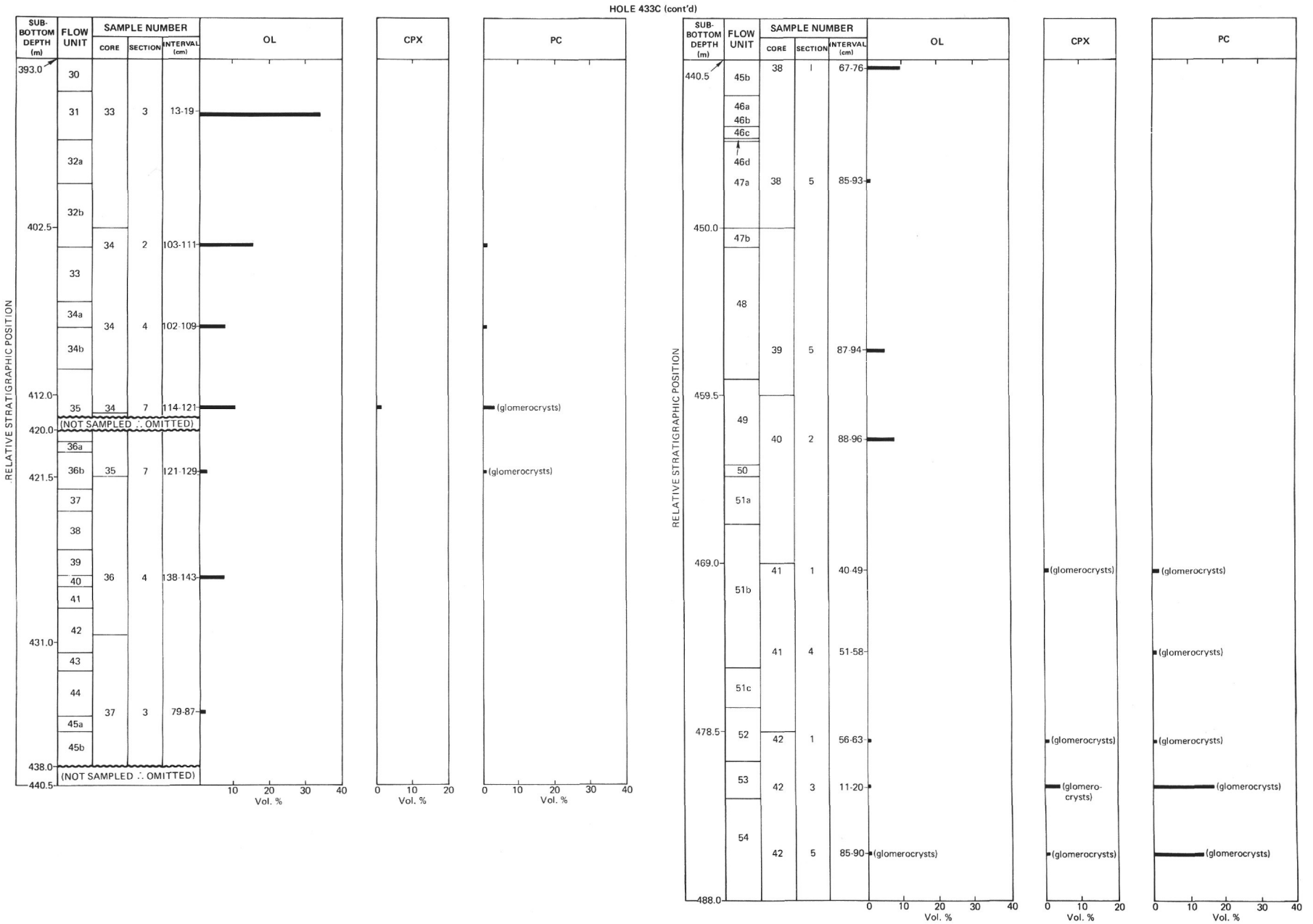

Figure 13. *(Continued).*

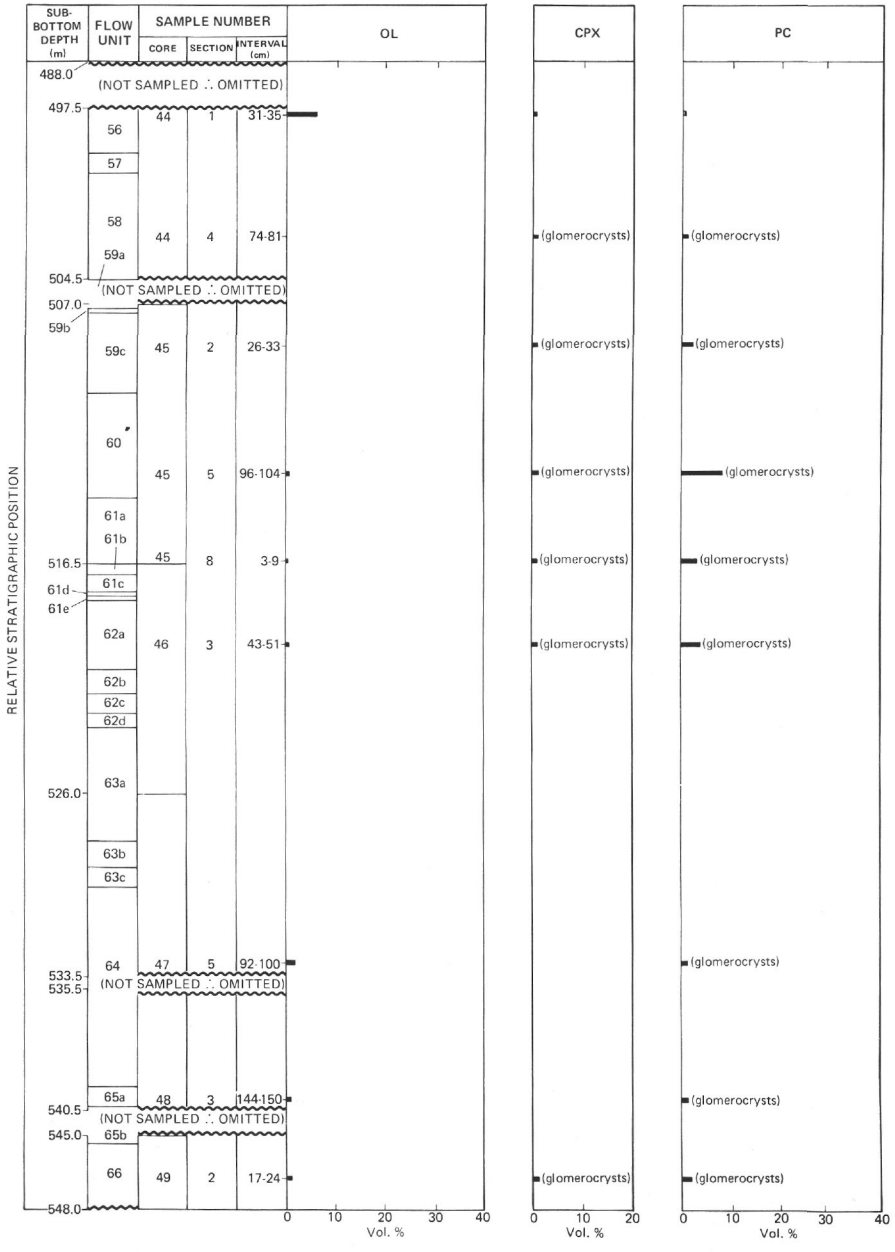

Figure 13. *(Continued).*

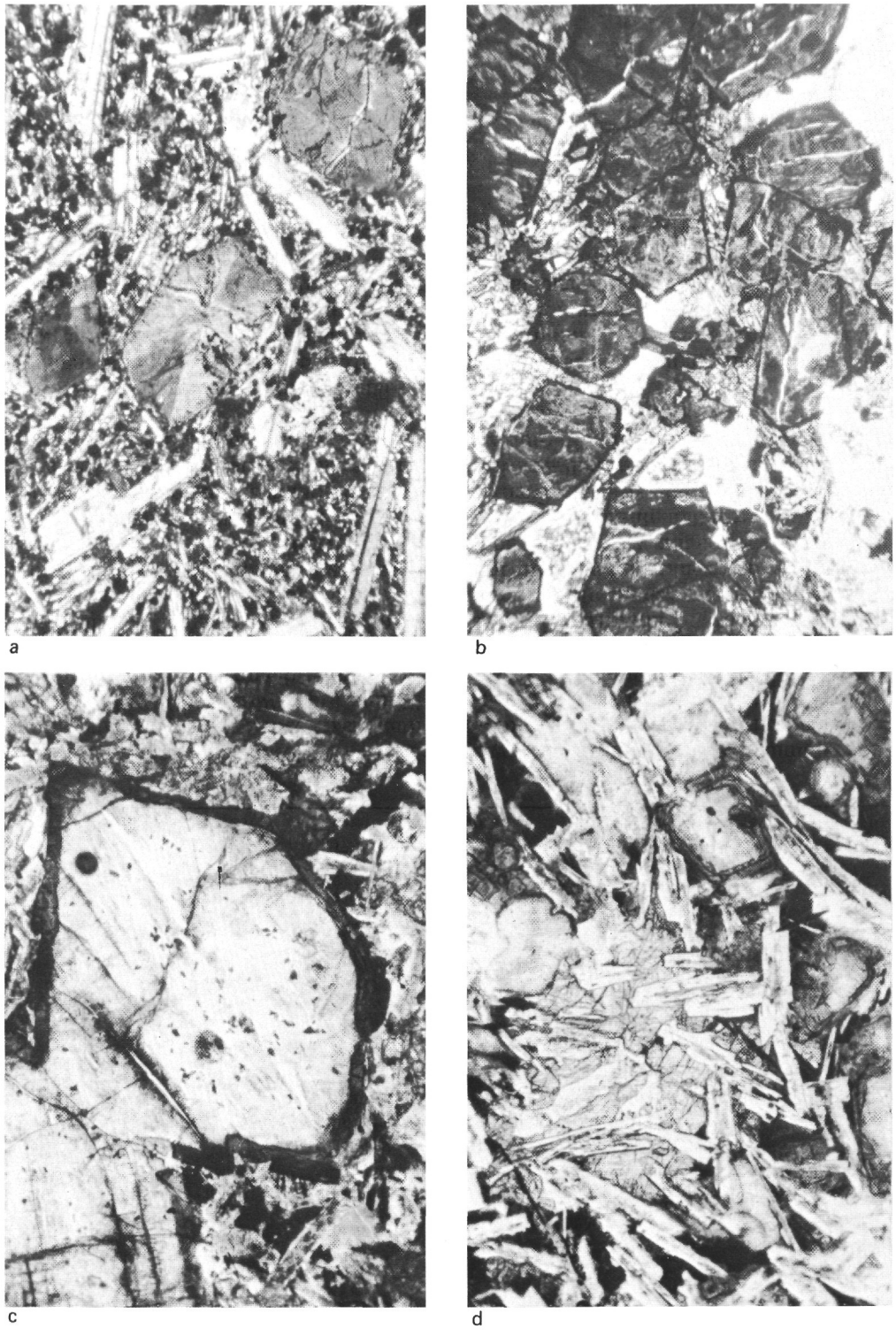

Figure 14. *Photomicrographs of Site 433 basalts. A) Sector-zoned pyroxene microphenocryst in intergranular textured alkalic basalt, Sample 433A-5-2, 83–85 cm. Plane light. Length of field is 1.3 mm. B) Cumulate olivine phenocrysts in picritic tholeiite. Rims of olivines are iddingsitized, centers are replaced by clay. Sample 433C-10-4, 118–120 cm. Plane light. Length of field is 4.9 mm. C) Cumulate olivine phenocryst in picritic tholeiite, showing iddingsitized rim and center altered to clay. Sample 433C-10-2, 15–18 cm. Plane light. Length of field is 1.3 mm. D) Ophitic texture in groundmass of tholeiitic basalt. Note groundmass olivine grain with iddingsitized rim and clay center. Sample 433C-26-6, 109–112 cm. Plane light. Length of field is 1.3 mm.*

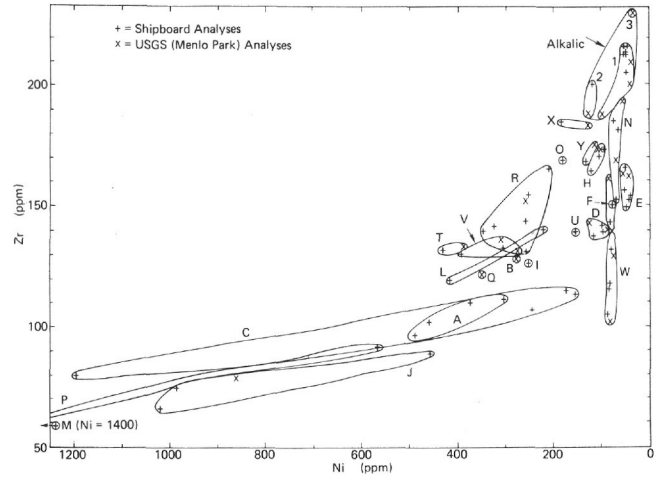

Figure 15. *Zr–Ni variation diagram for Site 433 tholeiitic basalts. Each group (A–Y) is chemically, mineralogically, and stratigraphically coherent.*

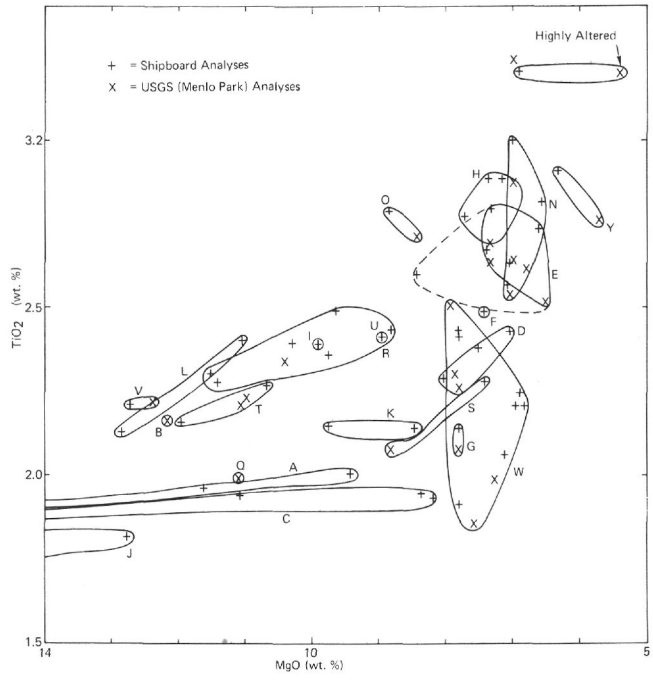

Figure 16. *TiO_2–MgO variation diagram for Site 433 tholeiitic basalts. The groups are the same as defined by Zr–Ni (Figure 15).*

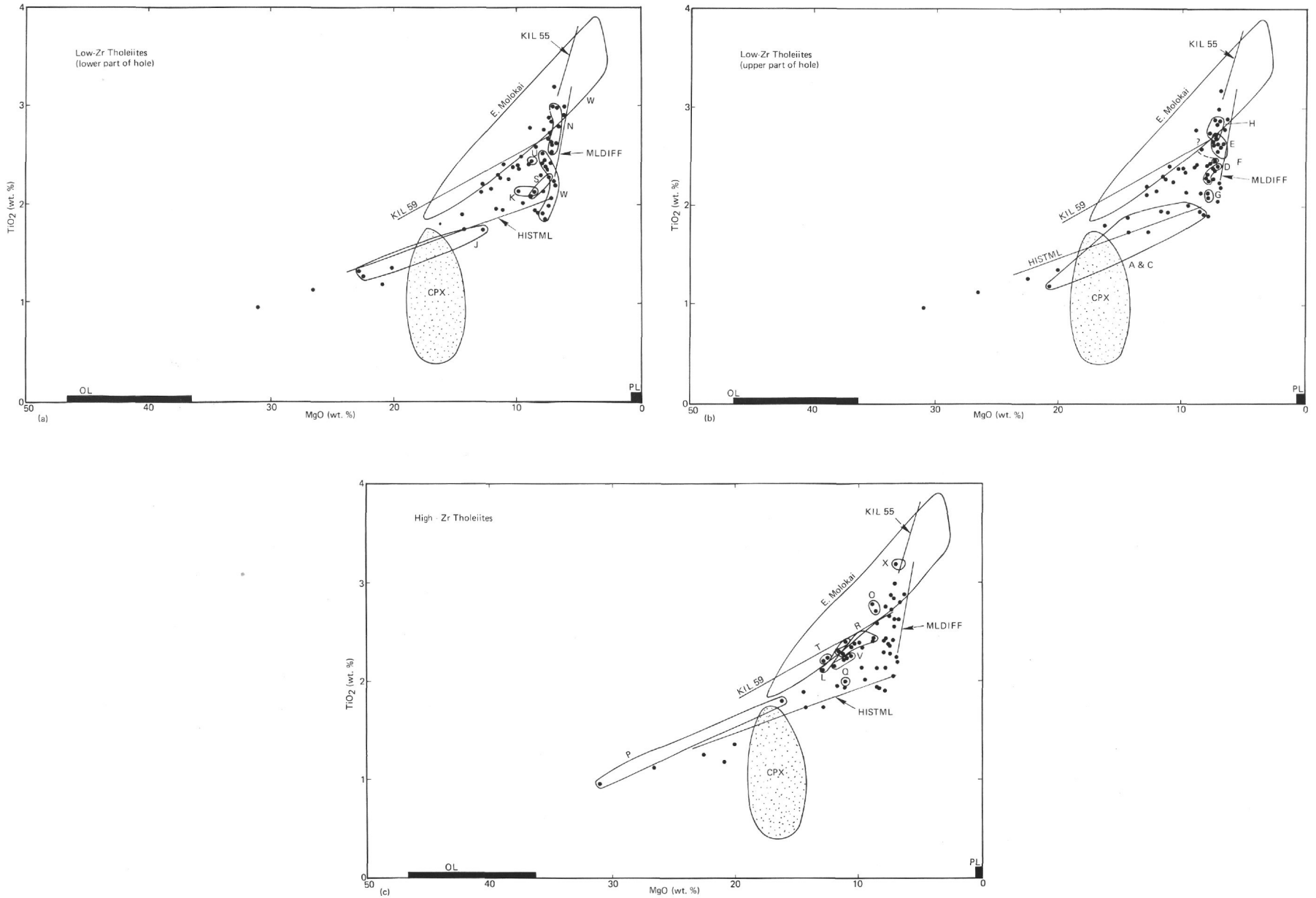

Figure 17. *Comparison of TiO_2-MgO compositional trends for tholeiitic basalts at Suiko Seamount (Site 433), Kilauea olivine-controlled trend (KIL59), Kilauea differentiated trend (KIL55), Mauna Loa olivine-controlled trend (HISTML), Mauna Loa differentiated trend (MLDIFF), and East Molokai trend. Suiko stratigraphic groups identified in Table 11 are indicated by lettered fields. Stippled field labeled CPX encloses clinopyroxene phenocryst compositions (Clague et al., this volume). a) and b) Suiko low-Zr types, c) Suiko high-Zr types.*

higher MgO values for the high-Zr type than for the low-Zr type.

It is not clear whether these two types of tholeiite are the product of one volcano alternately erupting two different types of lava or of two neighboring volcanoes contemporaneously erupting different lavas. The position of Site 433 on a neck between the main part of Suiko seamount and a northwestward projection which is quite likely a separate volcano (see 433 Site Report, this volume) suggests that we may have sampled a region of overlap between two volcanoes.

The occurrence of chemical and mineralogical groups within this sequence of flows is similar to the situation on East Molokai (Beeson, 1976), although the rock types and apparent fractionation trends there are different from those at Site 433. The East Molokai section is 305 meters thick, and is the only other well-studied section in the Hawaiian-Emperor chain with a thickness comparable to that at Hole 433C. At both Site 433 and East Molokai, the chemical variation within each group of one to a few flows is quite small with, perhaps, some indication of more fractionated compositions upward. At East Molokai, however, the overall trend for the entire section is toward more fractionated and alkali compositions upward. At Site 433 there is no overall trend. In addition, at East Molokai there appears to be a continuous trend from transitional tholeiitic compositions at the bottom to clearly alkalic compositions at the top. Beeson (1976) has proposed either high-pressure fractionation of aluminous pyroxene or varying partial fusion of mantle peridotite to account for this. At Site 433, the difference between the tholeiitic and alkalic basalts is much more distinct.

Fractionation and Origin of Basalts

Qualitatively, the overall compositional trends for the Site 433 tholeiitic basalts are similar to those observed on Kilauea and Mauna Loa volcanoes on the island of Hawaii (Wright, 1971; Wright and Fiske, 1971) and quite different from the trend for East Molokai (Beeson, 1976). As for most Hawaiian-Emperor chain suites, however, the trends are in detail different from any others. Figure 17 presents the compositional trends for the Site 433 tholeiites in terms of TiO_2-MgO, along with the Kilauea, Mauna Loa, and East Molokai trends. One of the Kilauea trends (KIL59) and the Mauna Loa trends (HISTML) are for olivine composition control (Wright, 1971). The other Kilauea trend (KIL55) involves olivine, clinopyroxene, and plagioclase (Wright and Fiske, 1971). The East Molokai trend apparently involves mantle processes (Beeson, 1976), although olivine, clinopyroxene, and plagioclase phenocrysts are present even in the most magnesian flows.

The compositions in the picrite and olivine phyric tholeiite groups from Site 433 — A and C (these two have similar magnetic inclinations and are probably related), J, P, R, and V — appear to be controlled by olivine alone. Although most of these flows are quite altered and their MgO content has probably been changed, their compositional trends extrapolate linearly back to the observed range of olivine phenocryst compositions. With two exceptions (Figure 18), these flows contain only olivine phenocrysts (up to 50%), and the more magnesian ones probably represent olivine accumulation. (Clague and Frey, this volume). As at Kilauea (Wright, 1971), each picritic group has somewhat different TiO_2 content for a given MgO content. This probably represents different depths of melting or a different mantle composition during the generation of each magma batch. The magnetic inclination within each picritic groups varies very little, indicating they were erupted within a short period (Kono, this volume). It seems likely that each is the result of a single magmatic event. Wright (1971) has shown that for Kilauea and Mauna Loa each of these magmatic events is the result of a new surge of magma entering the volcano from the mantle. At Kilauea in recent years, these events have occurred every few years (Wright, 1971). Given the small variation in magnetic inclination in the picrite groups, this may also have been the time scale for the duration of a magmatic event on Suiko.

As for the KIL55 trend (Wright and Fiske, 1971), the compositions of the olivine, clinopyroxene, and plagioclase phyric groups (D, E, F, G, H, I, K, N, O, U, W, X, and Y) probably reflect, in part, fractionation of these phases. It is highly unlikely, however, that the entire trend of these groups is a consequence of low-pressure fractionation of one or even a few parent magmas. As for the olivine phyric groups, the magnetic inclination in most of the multiply saturated groups varies little, indicating that the flows were erupted within a relatively few years. If the Kilauea model of Wright and Fiske (1971) is applicable, the chemical variation in each of these groups probably represents the effects of low-pressure processes (fractionation, magma mixing) superimposed on the initial composition of the magma as it came from the mantle. A few of the multiply saturated groups (D, E, H, N, W) do contain major magnetic inclination breaks, implying major time gaps. The most likely explanations for this are that the source region produced magma of similar composition at different times or that shallow fractionation brought the magma compositon to the same point twice in succession.

There are also major breaks in magnetic inclination between many of the chemical groups. These major changes (indicated by slashes in Table 10) probably also reflect long time intervals between flows, perhaps many thousands of years (Kono, this volume). If the time scale of a few years for a magmatic event is applicable to Suiko, each stratigraphic group represents one, or possibly two (if there is a break in magnetic inclination), separate events involving injection of magma from the mantle into the volcano.

These changes in magnetic inclination do not necessarily imply that the volcano was quiet for thousands of years, however, since the drill penetrates only one spot and lava must have flowed in all directions over the volcano to build up the shield.

The exact origin of the chemical variation within each of the groups is difficult to evaluate. The rocks are so

TABLE 8
Chemical Analyses and Norms of Volcanic Rocks from Site 433, Suiko Seamount

Hole	433A		433B	433C						
Core-Sec., Interval (cm)	20-1, 30-36	21-4, 129-138	5-3, 89-92	4-1, 25-30	6-2, 76-79	10-4, 11-17	12-3, 57-65	13-2, 55-66	14-3, 8-15	15-6, 16-31
Flow Unit	1	1	2	2	3	4F	9	10	11B	13
					As Received					
SiO_2	46.73	46.18	46.64	46.19	46.64	42.03	45.18	46.56	45.95	47.49
Al_2O_3	14.48	14.54	14.38	13.92	14.03	14.09	14.27	14.06	14.56	14.15
Fe_2O_3	6.84	7.87	5.13	4.13	7.04	9.38	4.78	4.36	6.78	5.14
FeO	7.13	6.45	8.29	9.46	7.62	3.51	6.17	7.74	6.34	8.03
MgO	5.32	5.22	6.50	7.63	5.09	11.01	7.46	7.50	6.96	6.65
CaO	9.44	9.16	9.51	9.46	8.83	6.16	11.60	10.49	8.68	10.31
Na_2O	3.51	3.48	3.24	3.06	3.63	2.29	2.77	2.63	2.96	2.88
K_2O	0.90	0.88	0.84	0.76	0.96	0.51	0.34	0.44	0.41	0.24
H_2O^+	0.77	1.06	1.37	1.19	1.22	3.98	1.26	1.68	1.49	0.59
H_2O^-	1.09	1.31	0.73	0.72	1.11	5.32	2.44	2.02	3.36	1.41
TiO_2	3.07	3.12	2.84	2.81	3.37	1.95	2.19	2.17	2.50	2.54
P_2O_5	0.42	0.34	0.37	0.38	0.44	0.19	0.23	0.24	0.25	0.27
MnO	0.18	0.17	0.18	0.18	0.23	0.11	0.20	0.16	0.11	0.16
CO_2	0.08	0.04	0.02	0.05	0.06	0.05	1.64	0.03	0.06	0.03
Total	99.96	99.82	100.04	99.94	100.27	100.58	100.53	100.08	100.41	99.89
					Dry Reduced Normalized					
SiO_2	48.01	47.79	47.88	47.34	48.00	46.55	47.70	48.54	48.46	48.78
Al_2O_3	14.88	15.05	14.76	14.27	14.44	15.60	15.07	14.66	15.36	14.54
FeO	13.65	14.01	13.25	13.51	14.36	13.24	11.06	12.16	13.12	13.00
MgO	5.47	5.40	6.67	7.82	5.24	12.19	7.88	7.82	7.34	6.83
CaO	9.70	9.48	9.76	9.70	9.09	6.82	12.25	10.94	9.15	10.59
Na_2O	3.61	3.60	3.33	3.14	3.74	2.54	2.92	2.74	3.12	2.96
K_2O	0.92	0.91	0.86	0.78	0.99	0.56	0.36	0.46	0.43	0.25
TiO_2	3.15	3.23	2.92	2.88	3.47	2.16	2.31	2.26	2.64	2.61
P_2O_5	0.43	0.35	0.38	0.39	0.45	0.21	0.24	0.25	0.26	0.28
MnO	0.18	0.18	0.18	0.18	0.24	0.12	0.21	0.17	0.12	0.16
					Norms ($Fe^{+3}/[Fe^{+3}+Fe^{+2}]$) = 0.15					
OR	5.42	5.36	5.07	4.60	5.84	3.30	2.12	2.71	2.54	1.47
AB	28.48	28.32	27.32	25.84	30.08	21.45	21.55	23.14	26.34	24.99
AN	21.63	22.16	22.74	22.49	19.64	29.45	26.90	26.29	26.58	25.59
NE	1.08	1.12	0.43	0.36	0.81	–	1.69	–	–	–
DI	19.55	18.66	19.02	18.84	18.64	2.39	26.24	21.47	13.98	20.58
DIWO	9.84	9.38	9.65	9.60	9.36	1.23	13.44	10.96	7.11	10.44
DIEN	4.69	4.40	5.03	5.26	4.29	0.77	7.86	6.14	3.83	5.48
DIFS	5.01	4.88	4.37	3.99	4.99	0.39	4.94	4.38	3.04	4.66
HY	–	–	–	–	–	12.04	–	7.23	10.65	11.32
HYEN	–	–	–	–	–	7.97	–	4.22	5.94	6.11
HYFS	–	–	–	–	–	4.07	–	3.01	4.72	5.20
FO	6.24	6.32	8.09	9.93	6.11	15.10	8.22	6.36	5.94	3.77
FA	7.34	7.74	7.71	8.32	7.83	8.50	5.68	5.00	5.20	3.54
MT	3.30	3.38	3.20	3.26	3.46	3.20	2.66	2.93	3.17	3.14
IL	5.97	6.12	5.53	5.46	6.57	4.09	4.38	4.28	5.00	4.95
AP	1.02	0.83	0.90	0.92	1.06	0.50	0.57	0.59	0.61	0.66
Total	100.02	100.02	100.02	100.02	100.03	100.01	100.02	100.02	100.02	100.02

highly altered that quantitative fractionation or mixing calculations (Wright and Doherty, 1970) would not be useful. Wright and Fiske (1971), however, have shown that for the fractionated lavas of Kilauea volcano the chemical variation within lavas of a single eruptive phase (comparable, we postulate, to each of our chemical groups) results from fractionation of the observed phenocryst phases and, to some extent, mixing of magmas from different events. The compositional trends within each of the groups on Suiko is in qualitative agreement with these causes. The exact composition of each group, then, reflects a combination of the composition of the mantle-derived parent magma and the extent of low-pressure fractionation.

The differences between the low-Zr and high-Zr tholeiites appear to be more fundamental. In addition to differences in the incompatable-element concentrations at a given MgO or Ni value, the two types begin crystallizing plagioclase and pyroxene at different MgO values, the high-Zr type at higher values (Figure 18). The slope of the compositional trend for the multiple saturated samples is also less for the high-Zr type than for the low-Zr type, implying that olivine or pyroxene are more important relative to plagioclase for the high-Zr type than they are for the low-Zr type. The origin of this difference is not clear. There appears to be no systematic difference in major-element oxides, includ- SiO_2, Al_2O_3, FeO, and CaO, which could account for this difference. The samples may, however, be so altered that subtle differences in one or more of these elements is masked by the alteration effects.

COMPOSITIONAL VARIATION ALONG THE HAWAIIAN-EMPEROR CHAIN

One of the major questions we set out to answer on Leg 55 was whether the compositions of the lavas erupted changed with position along the Hawaiian–Emperor chain. Knowledge of such change, if any, is essential to discussions of the long-term history of the Hawaiian hot spot, changes in the conditions of magma genesis, and changes in the source material from which the magma is derived.

TABLE 8 – *Continued*

433C										
17-1, 78–82 13	19-5, 57–65 15A	21-4, 7–13 17	22-5, 45–52 18	24-7, 133–139 19D	28-2, 73–80 25	29-1, 112–123 26A	29-2, 94–100 26B	29-1, 28–34 27	34-2, 103–111 33	34-7, 114–121 35
					As Received					
48.83	47.33	46.67	46.31	43.30	48.02	48.02	47.49	46.32	45.26	46.66
13.96	14.81	15.44	15.49	9.00	14.19	13.68	13.94	14.86	13.44	12.71
3.06	4.15	6.03	4.95	3.36	3.69	3.25	6.38	3.52	7.60	5.20
10.18	7.24	5.66	7.59	8.76	8.75	8.72	6.10	9.35	4.40	6.49
6.44	7.54	7.04	6.78	21.21	6.89	6.79	6.42	8.29	10.48	9.97
10.54	10.21	8.64	9.45	5.00	10.32	10.43	9.81	9.82	9.23	9.71
2.84	2.72	3.22	3.22	1.24	2.80	2.71	2.78	2.94	2.25	2.37
0.29	0.23	0.89	0.47	0.21	0.16	0.46	0.92	0.39	0.11	0.20
0.44	1.34	1.30	1.79	4.59	0.74	0.47	0.83	1.32	2.60	1.64
0.54	2.58	2.75	1.39	1.40	1.50	2.03	1.42	0.56	2.51	2.69
2.48	2.00	2.59	2.79	1.23	2.46	2.57	2.89	2.66	1.88	2.24
0.25	0.19	0.29	0.31	0.11	0.26	0.31	0.34	0.27	0.16	0.27
0.19	0.12	0.11	0.15	0.16	0.17	0.17	0.17	0.17	0.19	0.19
0.06	0.02	0.12	0.02	0.05	0.04	0.08	0.10	0.04	0.06	0.40
100.10	100.48	100.75	100.71	99.62	99.99	99.87	99.59	100.51	100.26	100.74
					Dry Reduced Normalized					
49.45	49.24	48.63	47.73	46.44	49.33	49.71	49.16	47.15	47.98	48.86
14.14	15.41	16.09	15.97	9.65	14.58	14.11	14.43	15.13	14.25	13.31
13.10	11.42	11.55	12.42	12.64	12.40	12.00	12.26	12.74	12.01	11.70
6.52	7.84	7.34	6.99	22.75	7.08	7.00	6.65	8.44	11.11	10.44
10.67	10.62	9.00	9.74	5.36	10.60	10.76	10.16	10.00	9.78	10.17
2.88	2.83	3.35	3.32	1.33	2.88	2.79	2.88	2.99	2.39	2.48
0.29	0.24	0.93	0.48	0.23	0.16	0.47	0.95	0.40	0.12	0.21
2.51	2.08	2.70	2.88	1.32	2.53	2.65	2.99	2.71	1.99	2.35
0.25	0.20	0.30	0.32	0.12	0.27	0.32	0.35	0.27	0.17	0.28
0.19	0.12	0.11	0.15	0.17	0.17	0.18	0.18	0.17	0.20	0.20
					Norms ($Fe^{+3}/[Fe^{+3}+Fe^{+2}]$) = 0.15					
1.71	1.42	5.48	2.83	1.36	0.94	2.78	5.63	2.36	0.71	1.24
24.32	23.90	28.29	28.03	11.23	24.32	23.73	24.42	25.25	20.18	21.06
24.74	28.58	26.07	27.20	19.64	26.33	24.58	23.69	26.62	27.74	24.68
–	–	–	–	–	–	–	–	–	–	–
21.82	18.54	13.50	15.52	4.88	20.02	21.92	20.10	17.24	15.86	19.46
11.04	9.48	6.90	7.91	2.55	10.18	11.18	10.24	8.82	8.17	10.05
5.62	5.43	3.96	4.33	1.81	5.52	6.25	5.66	5.06	5.08	6.37
5.15	3.63	2.64	3.29	0.52	4.31	4.49	4.19	3.36	2.60	3.04
15.24	12.21	2.55	1.66	23.64	15.79	15.98	10.77	1.38	13.61	16.95
7.96	7.38	1.53	0.94	18.40	8.86	9.30	6.19	0.83	9.00	11.47
7.28	4.89	1.02	0.78	5.23	6.93	6.68	4.58	0.55	4.61	5.48
1.84	4.72	8.94	8.48	25.45	2.25	1.34	3.32	10.57	9.49	5.76
1.85	3.48	6.57	7.09	7.98	1.94	1.06	2.71	7.75	5.36	3.03
3.15	2.75	2.80	3.00	3.05	3.00	2.82	2.86	3.07	2.89	2.71
4.76	3.94	5.12	5.46	2.50	4.80	5.04	5.69	5.14	3.77	4.46
0.59	0.47	0.71	0.76	0.28	0.64	0.76	0.83	0.64	0.40	0.67
100.02	100.01	100.02	100.02	100.01	100.02	100.02	100.02	100.02	100.01	100.02

Because of their abundance and simple phenocryst mineralogy, we have chosen to use olivine + chromite phyric tholeiitic basalts to make this comparison. This is because it is possible to normalize analyses of this rock type to a constant Mg/(Mg + Fe) value by olivine fractionation only. This, then, allows comparison of lavas from different volcanoes at the same stage of fractionation, assuming that olivine has been the only significant fractionating phase since the magma was formed and that olivine is always left as a residual phase after partial melting. If mineralogical descriptions are not given in the original references, we have used only analyses with MgO content greater than 8 per cent. These, in our experience, have almost always only olivine + chromite phenocrysts.

The normalizations were carried out by averaging the selected dry reduced analyses for each volcano and adding or subtracting olivine with the composition Fo_{86} to give $Mg/(Mg + 0.85\ Fe_T) = 0.70$. These calculated magma compositions should be in equilibrium with mantle olivine if $K_{Mg} = 0.3$ (Roeder and Emslie, 1970). $Fe^{+2} = 0.85\ Fe_T$ gives roughly the Fe^{+2}/Fe^{+3} ratio of the least oxidized tholeiitic basalts of Kilauea and Mauna Loa (Wright, 1971). Fo_{86} is a good average for the olivine phenocryst compositions in this rock type. We do not propose that the normalized average compositions represent original parental magmas, although they could be fairly close. Our objective is only to compare rocks from different volcanoes under conditions as similar as possible.

Table 11 presents the averaged and normalized dry reduced compositions for each volcano for which data are available. Table 12 presents the averaged as received analyses for the various rock types from the Leg 55 drill sites.

The principal conclusion to be drawn from Table 11 is that there appear to be no systematic changes in any of the major elements for olivine tholeiites along the chain from Kilauea to Suiko. There are large differences in many of the elements from volcano to volcano (TiO_2 for Kilauea and Mauna Loa) and even for different types at the same volcano (high-TiO_2 and low-

TABLE 8 – *Continued*

Hole	433C								
Core-Sec., Interval (cm) Flow Unit	37-3, 79-87 44	38-1, 67-76 45B	39-5, 87-94 48	40-2, 88-96 49	42-1, 56-63 52	42-3, 11-20 53	42-5, 85-92 54	47-5, 92-100 64	49-2, 17-24 66
				As Received					
SiO_2	47.57	44.80	47.28	47.32	47.75	47.39	47.91	44.10	45.34
Al_2O_3	13.81	13.25	12.82	12.61	13.25	15.97	14.76	14.51	15.41
Fe_2O_3	3.63	3.67	2.51	3.90	4.78	4.58	4.20	11.01	9.22
FeO	7.72	8.69	9.17	7.90	7.41	5.62	6.92	3.37	4.16
MgO	8.49	11.79	10.62	10.73	7.57	7.22	7.04	5.09	5.73
CaO	10.28	7.95	9.50	9.68	9.77	10.04	11.24	9.23	9.14
Na_2O	2.48	2.36	2.15	2.36	2.50	2.84	2.46	3.08	3.08
K_2O	0.16	0.45	0.21	0.21	0.31	0.23	0.16	1.51	0.54
H_2O^+	1.33	3.30	1.75	1.73	0.76	1.35	0.47	1.78	1.87
H_2O^-	2.27	1.46	1.10	1.00	2.84	3.45	2.24	2.25	3.19
TiO_2	2.00	2.11	2.15	2.14	2.40	1.77	1.92	3.02	2.76
P_2O_5	0.19	0.20	0.23	0.25	0.22	0.15	0.18	0.32	0.30
MnO	0.17	0.16	0.17	0.17	0.13	0.12	0.13	0.16	0.16
CO_2	0.03	0.04	0.05	0.07	0.10	0.04	0.09	0.51	0.09
Total	100.14	100.23	99.71	100.07	99.79	100.77	99.72	99.94	100.99
				Dry Reduced Normalized					
SiO_2	49.48	47.13	48.96	48.84	49.94	49.64	49.65	46.77	47.77
Al_2O_3	14.36	13.94	13.28	13.02	13.86	16.73	15.30	15.39	16.24
FeO	11.43	12.62	11.85	11.78	12.26	10.20	11.09	14.08	13.13
MgO	8.83	12.40	11.00	11.08	7.92	7.56	7.30	5.40	6.04
CaO	10.69	8.36	9.84	9.99	10.22	10.52	11.65	9.79	9.63
Na_2O	2.58	2.48	2.23	2.44	2.61	2.97	2.55	3.27	3.24
K_2O	0.17	0.47	0.22	0.22	0.32	0.24	0.17	1.60	0.57
TiO_2	2.08	2.22	2.23	2.21	2.51	1.85	1.99	3.20	2.91
P_2O_5	0.20	0.21	0.24	0.26	0.23	0.16	0.19	0.34	0.32
MnO	0.18	0.17	0.18	0.18	0.14	0.13	0.13	0.17	0.17
				Norms $(Fe^{+3}/[Fe^{+3}+Fe^{+2}]) = 0.15$					
OR	1.00	2.77	1.30	1.30	1.90	1.42	1.01	9.43	3.36
AB	21.79	20.94	21.95	20.68	22.16	25.09	21.62	20.45	27.35
AN	27.04	25.46	23.86	23.96	25.24	31.56	29.86	22.53	28.02
NE	–	–	–	–	–	–	–	3.87	–
DI	20.00	11.77	18.81	19.38	19.68	15.89	21.89	19.68	14.50
DIWO	10.26	6.08	9.72	10.01	10.07	8.14	11.19	9.90	7.33
DIEN	6.09	3.86	6.17	6.38	5.83	4.78	6.41	4.62	3.69
DIFS	3.65	1.83	2.92	2.99	3.78	2.97	4.30	5.17	3.48
HY	16.70	9.35	14.30	16.36	22.44	11.62	16.35	–	4.44
HYEN	10.44	6.35	9.70	11.14	13.61	7.17	9.79	–	2.28
HYFS	6.26	3.01	4.60	5.22	8.83	4.46	6.56	–	2.16
FO	3.79	14.44	8.04	7.09	0.25	4.80	1.41	6.17	6.33
FA	2.50	7.53	4.20	3.66	0.18	3.29	1.04	7.62	6.58
MT	2.76	3.04	2.77	2.76	2.84	2.46	2.59	3.40	3.17
IL	3.94	4.21	4.22	4.20	4.78	3.51	3.79	6.06	5.51
AP	0.47	0.50	0.57	0.62	0.55	0.38	0.45	0.80	0.76
Total	100.01	100.01	100.02	100.02	100.01	100.01	100.01	100.02	100.02

Notes: 1 – Cl analyses on 433A-21-4, 129–138 cm; 433C-13-2, 55–66 cm; 433C-14-3, 8–15 cm; 433C-15-6, 16–31 cm; 433-17-1, 78–82 cm; 433C-28-2, 73–80 cm; 433C-47-5, 92–100 cm; and 433C-49-2, 17–24 cm gave <0.05%.

TiO_2 types at Suiko), but there are no uniform changes along the chain. The only possible systematic difference is that the lavas from Nihoa (7 m.y.B.P.) to Daikakuji (45 m.y.B.P.) may have lower Al_2O_3 and higher TiO_2 contents than those before (Suiko) and after (Niihau to Kilauea).

This lack of variation in major-element compositions is in good agreement with the lack of systematic variation in incompatible trace element ratios found by Clague and Frey (this volume). Subtle variations like the decrease in initial strontium isotope ratios from the Hawaii-Emperor bend to Suiko found by Lanphere et al. (this volume) are probably beyond the resolution of our averaging and normalizing procedure.

SPECULATION ON THE ORIGIN OF THE HAWAIIAN-EMPEROR MAGMA

The lack of systematic variation in the major and trace elements along the chain, discussed above and by Clague and Frey (this volume), implies that the conditions of magma genesis, the composition of the parental material, and the extent of melting at the Hawaiian hot spot have not changed significantly since Suiko was formed. There have clearly been fluctuations in at least one of these, but mostly they appear to be relatively short-lived. Kilauea and Mauna Loa lavas, for instance, are significantly different, but both volcanoes are presently active. The CaO and TiO_2 anomalies for Nihoa to Daikakuji may represent a longer term fluctuation in source composition. The major problem, however, is how to account for the overall stability.

If the Hawaiian hot spot is to be relatively fixed (and the magnetic evidence from Suiko [Kono, this volume] indicates that at least the change in latitude has not been great), the heat source for the igneous activity must be at least as deep as the asthenosphere and possibly deeper. It is very unlikely that it is in the lithosphere, since the lithosphere in the Pacific appears to be in motion away from the east Pacific rise.

The evidence for the ultimate location of the magma's source material is considerably weaker. The lines of evidence we have are that (1) the depth of melting to produce the parental tholeiitic magma must

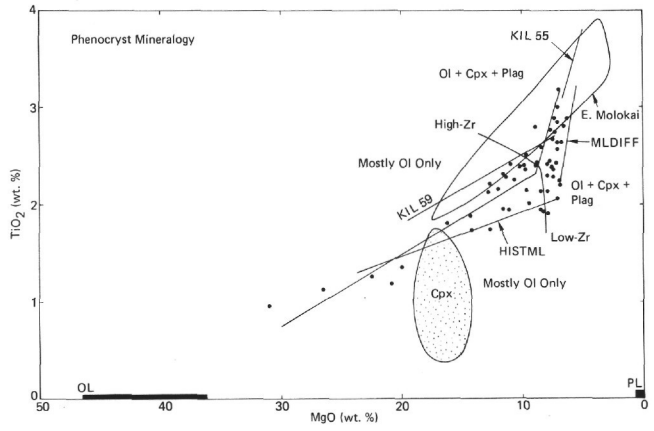

Figure 18. *Phenocryst phases present in Site 433 tholeiitic basalts versus position in TiO_2-MgO for both high-Zr and low-Zr types.*

TABLE 9
Trace-Element Analyses of Lava Flows from Suiko Seamount, DSDP Site 433

Hole	Core-Section, Interval (cm)	Flow Unit	Concentrations (ppm) Ba	Cr	Ni	Sr	Zn	Zr	Y
433A	20-1, 30-36	1	295	<100	41	390	143	200	44
433A	21-4, 129-138	1	270	<100	40	380	135	210	37
433B	5-3, 89-92	1	250	<100	95	360	112	188	28
433C	4-1, 25-28	2	245	<100	126	345	125	188	30
433C	6-2, 76-79	3	305	<100	36	360	152	230	36
433C	10-4, 11-17	4F	174	<100	275	200	121	129	27
433C	12-3, 57-65	9	107	<100	127	305	128	143	27
433C	13-2, 55-66	10	144	224	89	245	85	140	12
433C	14-3, 8-15	11B	87	116	43	285	116	162	32
433C	15-6, 16-31	13	95	110	56	290	117	163	25
433C	19-5, 57-65	15A	178	250	101	275	101	127	27
433C	21-4, 7-13	17	163	172	106	340	150	173	30
433C	22-5, 45-52	18	156	186	99	350	117	173	35
433C	24-7, 133-139	19D	70	390	860	87	128	79	21
433C	29-1, 112-123	26A	101	<100	70	300	113	169	33
433C	29-2, 94-100	26B	98	<100	61	305	128	194	33
433C	34-2, 103-111	33	79	470	350	240	99	121	23
433C	34-7, 114-121	35	98	385	260	280	114	151	31
433C	37-3,79-87	44	66	310	142	96	<5	111	<9
433C	38-1, 67-76	45B	94	440	385	260	119	133	28
433C	39-5, 87-94	48	99	410	270	150	114	131	24
433C	40-2, 88-96	49	98	410	310	235	111	137	34
433C	42-1, 56-63	52	85	235	82	260	112	156	46
433C	42-3, 11-20	53	63	255	81	265	87	101	31
433C	42-5, 85-92	54	64	255	76	250	70	129	21
433C	47-5, 92-100	64	118	270	127	270	113	183	41
433C	49-2, 17-24	66	215	113	111	320	123	175	33

be relatively constant and probably fairly shallow, or there would not be tholeiitic basalts (Green and Ringwood, 1967); (2) the source material must be fairly uniform through time and must be continually replenished, or the magma composition would change and igneous activity would eventually stop; and (3) on the basis of seismic activity progressing to volcanism, the magma apparently enters conduits at a depth of at least 60 km (Wright, 1971). Because this depth is in the lithosphere, the source region could be in the lower lithosphere or asthenosphere. We do not have criteria to unambiguously distinguish these possibilities.

There are at least two physical pictures which are consistent with the data and with a heat source in the asthenosphere. The first is that material from the asthenosphere rises into the lower lithosphere where the melt separates from the residual crystals and rises to form the volcanoes. The other physical picture is that there is a more or less fixed and continuously operating heat source in the asthenosphere (diapirs or a plume, perhaps) which heats and partially melts the lower lithosphere as it passes over. The melt then separates from the residual crystals, enters a conduit system, and finally erupts to form the volcanoes.

In either of these pictures minor differences in magma compositon between volcanoes or even at one volcano can be accounted for by small variations in the source compositon, volatile content, fraction of melting, or depth of separation from the residual crystals.

Other physical pictures are also possible, and we do not mean to exclude them. Any other models must, however, be able to account for the data presented in this volume.

ACKNOWLEDGMENTS

The analyses reported here were done by N. H. Elsheimer, L. F. Espos, and S. T. Neil of the U. S. Geological Survey, Menlo Park. Their efforts are greatly appreciated. We also wish to thank Brent Dalrymple for many useful discussions and his help in preparing this paper. Most of all we wish to thank Dale Jackson, without whom this paper and this volume would not have been possible. Would that he were here.

REFERENCES

Bargar, K. E. and Jackson, E. D., 1974. Calculated volumes of individual shield volcanoes along the Hawaiian-Emperor chain, *Jour. Research U. S. Geol. Survey,* v. 2, pp. 545–550.

Beeson, M. H., 1976. Petrology, Mineralogy, and Geochemistry of the East Molokai Volcanic Series, Hawaii, *U. S. Geol. Surv. Prof. Paper 961,* U. S. Government Printing Office, Washington, 53 pp.

Bonhommet, N., Beeson, M. H., and Dalrymple, G. B., 1977. A contribution to the Geochronology and Petrology of the Island of Lanai, Hawaii, *Geol. Soc. Am. Bull.,* v. 88, pp. 1282–1286.

Dalrymple, G. B., Lanphere, M. A., and Jackson, E. D., 1974. Contributions to the petrography and geochronology of volcanic rocks from the Leeward Hawaiian Islands, *Geol. Soc. Am. Bull.,* v. 85, pp. 727–738.

Green, D. H., and Ringwood, A. E., 1967. The genesis of basaltic magmas, *Contr. Min. Pet.,* v. 15, pp. 103–190.

Macdonald, G. A., 1968. Composition and origin of Hawaiian lava, *Geol. Soc. Am. Mem.,* v. 116, pp. 477–522.

Macdonald, G. A., and Katsura, T., 1964. Chemical composition of Hawaiian lavas, *J. Petrol.,* v. 5, pp. 82–133.

Muir, I. D. and Tilley, C. E., 1961. Mugearites and their place in alkali igneous rock series, *J. Geol.,* v. 69, pp. 186–203.

Roeder, P. L. and Emslie, R. F., 1970. Olivine-liquid equilibrium, *Contr. Min. Pet.,* v. 29, pp. 275–289.

Wright, T. L., 1971. Chemistry of Kilauea and Mauna Loa lavas in time and space, *U. S. Geol. Survey Prof. Paper 735,* 40 pp.

Wright, T. L., and Doherty, P. C., 1970. A linear programming and least squares computer method of solving petrologic mixing problems, *Geol. Soc. Am. Bull.,* v. 81, pp. 1995–2008.

Wright, T. L., and Fiske, R. S., 1971. Origin of the differentiated and hybrid lavas of Kilauea volcano, Hawaii, *J. Petrol.,* v. 12, pp. 1–65.

TABLE 10
Stratigraphy of Tholeiitic Basalts, Hole 433C

Strat. Group	Chemical Type	Flow Units	Range (Core-Sec., Interval [cm])	Depth (m)	Phenocrysts	Magnetic[a] Unit	Comments
A	Low Zr	4a,4b,4c, 4d,4e	10 (top)- 10-3, 150	203- 208	Ol	2	Groups A and C may be the same unit separated by a stray flow from another source.
B	Hi Zr	4f	10-4, 0- 10-4, 65	208- 211	Ol	2	
C	Low Zr	4g,4h 5,6,7	10-4, 65- 11-4, 15	211- 218.5	Ol	2	
D	Low Zr	8,9,10	11-4, 15- 13-3, 60	218.5- 233	Ol,Pl,Cpx	– 3,4/5	
E	Low Zr	11b,11c, 12,13	14-1, 0- 19-1, 55	242.5- 262	Ol,Pl,Cpx	– 6/7	11a and 11d not analyzed.
F	Low Zr	14	19-1, 55- 19-1, 145	262- 264.5	Ol,Pl,Cpx	8	
G	Low Zr	15a	19-2, 145- 20-1, 60	264.5- 272	Ol,Pl,Cpx	– 9	15b not analyzed.
H	Low Zr	16,17,18	20-2, 80- 22-6, 15	272- 297.5	Ol,Pl,Cpx	– 10/11	
I	Hi Zr	19a	23-1, 0- 23-1, 120	297.5- 299	Ol,Cpx	12	19b not analyzed.
J	Low Zr	19c,19d	23-4, 40- 25-1, 65	303- 317.5	Ol	12	
K	Low Zr	20,21	25-1, 65- 26-3, 95	317.5- 330.5	Ol (Pl–trace)	12,13	
L	Hi Zr	22,23	26-3, 95- 26-7, 20	330.5- 336	Ol	14	Groups L and M may be same unit, M more 01-rich.
M	Hi Zr	24a	26-7, 20- 27-3, 75	336- 340	Ol	15	24b not analyzed.
N	Low Zr	25,26a,26b	27-6, 35- 29-3, 75	344- 359	Ol,Pl,Cpx	– 16/17	
O	Hi Zr	27	29-3, 75- 31-2, 55	359- 376	Ol,Pl,Cpx	– 18	
P	Hi Zr	28c,29	31-2, 55- 32-5, 130	376- 391	Ol	– 19,20	28a,b,d,30,31,32 not analyzed.
Q	Hi Zr	33	34-1, 110- 34-3, 120	403.5- 406.5	Ol	22	34 not analyzed.
R	Hi Zr	35,37, 38,39,41	34-6, 50- 36-5, 145	411.5- 429	Ol (F.U. 35–Ol, Pl,Cpx)	23,24,25	36,40,42,43 not analyzed.
S	Low Zr	44	37-2, 0- 37-4, 115	432- 436.5	Ol	26	
T	Hi Zr	45	37-4, 115- 38-2, 50	436.5- 442.5	Ol	27	46 not analyzed.
U	Low Zr	47	38-4, 10- 39-1, 115	445- 451.5	aphyric	– 28	
V	Hi Zr	48,49	39-1, 115- 40-3, 90	451.5- 463.5	Ol (48–trace Pl)	– 29	50 not analyzed.
W	Low Zr	51b,52, 53,54,60 62a	40-5, 113- 46-3, 140	467- 521	Ol,Pl,Cpx (51,52,53 essentially aphyric)	– 30,31, 32/35, 36	51a,51c,55,56,57,58,59,61,62b-d, 63 not analyzed
X	Hi Zr	64	47-2, 45- 48-3, 100	530- 539.5	Ol,Pl,Cpx	– 37	65 not analyzed.
Y	Low Zr	66	49-1, 30- 50-1, 50	545-?	aphyric	37	

[a] / or – indicate major jump in inclination (10–40°).

TABLE 11
Average Olivine Tholeiite Composition for Volcanoes of the Hawaiian-Emperor Chain[a]

	Kilauea	Mauna Loa	Manua Kea	Kohala	Haleakala	W. Maui	Lanai	E. Molokai	W. Molokai	Koolau	Waianae (upper)	Waianae (lower)
SiO_2	48.9	50.5	46.4	48.2	49.7	47.3	49.0	46.4	49.2	51.5	46.9	47.9
Al_2O_3	12.1	12.2	12.8	13.5	13.25	12.6	12.8	12.9	11.8	13.2	13.4	14.1
FeO	11.4	11.0	12.3	11.8	10.9	12.2	11.0	12.4	11.9	10.4	11.9	11.2
MgO	12.7	12.3	13.6	13.1	12.1	13.7	12.3	13.8	13.2	11.7	13.2	12.5
CaO	9.7	9.2	9.9	9.4	9.6	9.8	8.8	9.7	8.9	8.3	9.1	9.6
Na_2O	1.99	1.98	1.82	1.62	1.76	1.66	2.13	1.89	2.42	2.47	2.07	1.86
K_2O	0.44	0.36	0.28	0.10	0.33	0.23	0.11	0.20	0.18	0.27	0.53	0.26
TiO_2	2.34	1.85	2.40	1.93	2.01	2.14	1.66	2.22	2.08	1.68	2.46	2.20
P_2O_5	0.22	0.21	0.23	0.20	0.13	0.20	0.18	0.25	–	0.22	0.35	0.25
MnO	0.17	0.16	0.17	0.18	0.18	0.17	0.14	0.18	0.19	0.15	0.15	0.17

	Kauai	Niihau	Nihoa	#20	#21	Necker	La Perouse	North-ampton[b]	Pioneer	#63	Daikakuji	Suiko High TiO_2	Suiko Low TiO_2
SiO_2	48.4	48.4	47.4	46.85	47.1	47.15	47.5	48.7	48.15	46.5	49.7	47.6	47.9
Al_2O_3	12.5	12.1	11.5	11.2	11.3	11.1	11.7	11.4	11.2	11.4	11.5	12.7	13.0
FeO	11.9	12.1	12.4	13.6	12.4	12.8	11.8	11.7	11.9	12.8	11.5	12.3	11.9
MgO	13.3	12.6	13.8	14.0	13.8	14.1	13.1	13.0	13.3	14.2	12.9	13.7	13.2
CaO	9.2	8.1	9.4	9.6	9.2	9.8	10.7	10.05	9.8	8.4	9.05	8.7	9.3
Na_2O	1.93	2.28	1.77	2.06	2.25	1.59	1.82	2.00	2.20	2.75	2.08	2.26	2.26
K_2O	0.30	0.49	0.26	0.24	0.64	0.38	0.39	0.32	0.67	0.56	0.43	0.28	0.14
TiO_2	2.06	2.49	2.59	2.97	2.72	2.47	2.44	2.26	2.36	2.92	2.32	2.10	1.86
P_2O_5	0.23	0.31	(0.70)[c]	0.28	0.35	0.36	0.34	0.23	0.17	0.26	0.36	0.22	0.16
MnO	0.17	0.16	0.15	0.15	0.15	0.17	0.20	0.16	0.14	0.17	0.16	0.18	0.18

[a]Data are arranged as a function of distance from Kilauea. Volcano numbers of Bargar et al. (1974) are used for unnamed seamounts. Compositions are averages of dry reduced, normalized analyses of tholeiitic basalts with MgO=8%. Olivine (Fo_{86}) was added or subtracted so that 100Mg/(Mg+0.85Fe)=70.

[b]Data from M. O. Garcia, personal communication, 1978.

[c]Probably phosphatized.

Data for this table comes from Beeson, 1976; Bonhommet et al., 1977; Dalrymple et al., 1974; Macdonald, 1968; Macdonald and Katsura, 1964; Muir and Tilley, 1961; Wright, 1971; Wright and Fiske, 1971; and unpublished data of M. H. Beeson, D. Clague, and E. D. Jackson.

TABLE 12
Average Chemical Analyses of Lavas Recovered on Leg 55

	Ōjin Seamount (Site 430)		Nintoku Seamount (Site 432)	Suiko Seamount (Site 433)				
	Hawaiite	Tholeiite	Alkalic Basalt	Alkalic Basalt	Picritic Tholeiite	Olivine Tholeiite	Plagioclase Tholeiite	Tholeiite
SiO_2	47.8	47.7	46.3	46.5	43.3	45.7	47.2	46.6
Al_2O_3	15.9	15.3	16.5	14.3	9.0	13.4	14.6	14.3
Fe_2O_3	8.0	4.5	6.3	6.2	3.4	5.1	4.7	6.0
FeO	4.1	7.9	6.2	7.8	8.8	7.1	7.2	6.6
MgO	3.8	5.6	5.1	5.9	21.2	10.4	7.0	6.8
CaO	6.6	11.0	8.6	9.3	5.0	8.9	10.1	9.9
Na_2O	4.3	3.0	3.6	3.4	1.2	2.4	2.8	2.9
K_2O	1.7	0.36	1.2	0.87	0.21	0.30	0.39	0.54
H_2O^+	1.2	0.39	1.5	1.1	4.6	2.3	1.1	1.2
H_2O^-	2.1	1.0	1.3	1.0	1.4	2.1	2.2	2.2
TiO_2	2.9	2.8	2.7	3.0	1.2	2.2	2.3	2.5
P_2O_5	1.2	0.30	0.50	0.39	0.11	0.22	0.25	0.26
MnO	0.10	0.18	0.15	0.19	0.16	0.17	0.14	0.16
CO_2	0.06	0.04	0.10	0.05	0.05	0.10	0.05	0.32
Total	99.8	100.1	100.0	100.0	99.6	100.4	100.0	100.3

APPENDIX
Petrographic Summary for Site 433 Basalts

				Phenocrysts & Microphenocrysts			Vesicles				Groundmass
Hole	Core-Section, Interval (cm)	Flow Unit	Rock Type	Mineral	Per cent	Average Size (mm)	Per cent	Size Range (mm)	Average Size (mm)	Shape	Per cent
433A	20-1, 30–36	1	Alkalic Basalt	pl	4	0.62					95+
				ol	<1	0.58					
				cpx	<1	0.51					
	21-2, 86–90	1	Alkalic Basalt	pl	12	3.13					83
				cpx	4	0.97					
				ol	1	0.55					
	21-3, 115–123	1	Alkalic Basalt	pl	6	1.25	1	0.70–1.70	0.81	ovoid	92
				cpx	1	.62					
				ol	1	1.29					
	21-4, 129–138	1	Alkalic Basalt	pl	12	2.18	4	0.32–1.50	0.80	ovoid	83+
				cpx	4	0.54					
				ol	<1	0.55					
433B	5-2, 61–68	1	Alkalic Basalt	pl	3	1.35	1	0.15–0.41	0.32	ovoid	95
				cpx	2	0.56					
				ol	<1	0.70					
	5-3, 85–90	2	Alkalic Basalt	pl	9	1.00					81+
				ol	7	1.51					
				cpx	2	0.73					
433C	4-1, 30–38	2	Alkalic Basalt	pl	12	1.44					78+
				ol	7	2.16					
				cpx	2	1.15					
				mt	<1	0.46					
433C	5-1, 2–9	2	Alkalic Basalt	ol	7	2.40					82
				pl	7	1.71					
				cpx	4	1.50					

APPENDIX – *Continued*

Groundmass						
Dominant Texture	Size Range (mm)	Minerals[a]	Per cent	Opaque Minerals	Alteration and Remarks[b]	Other Work
microlitic, intergranular	0.02 –0.10 0.01 –0.05 0.001–0.02 0.01 –0.08	pl cpx mt ol	50–55 20–25 10–12 8–10	Equant timag., with ilmenite exsolution lamellae.	10–12% altered, ol completely replaced by smectite. Smectite has basal d=13.18Å which expands to 16.98Å after glycol. Mainly smectite A but trace of chlorite(?) and B also. Sector zoned cpx.	X,T,S,K,M
subtrachytic	0.02 –1.20 0.006–0.50 0.005–0.15 0.01 –0.50 0.01 –0.17	pl cpx mt ol il	57 18 4 3 1		10% altered, ol completely replaced by calcite and smectite. Smectite has basal d= 13.59Å which expands to 16.98Å after glycol. Mainly smectite A but trace of B also. Sector zoned cpx.	
subtrachytic	0.05 –0.90 0.01 –0.50 0.002–0.18 0.02 –0.50 0.01 –0.15	pl cpx mt ol il	57 23 6 5 1		12% altered, ol completely replaced by smectite. Smectite has basal d=12.80Å which expands to 17.31Å after glycol. Mainly smectite A but trace of B and chlorite(?) also. Sector zoned cpx.	
intergranular	0.05 –1.50 0.01 –0.50 0.002–0.25 0.01 –0.50 0.008–0.20 0.01 –0.15	pl cpx mt ol il ap	38 31 6 4 2 2	Equant timag. and equant ilmenite. Pyrite is present. Olivine phenocrysts contain chromite.	14% altered, ol completely replaced by smectite and iddingsite. Smectite has a basal d=14.02Å which expands to 16.98Å after glycol. Vesicles filled with fibrous olive-green smectite. Sector zoned cpx.	W,X,T,S, K,M
subtrachytic	0.05 –0.90 0.006–0.50 0.001–0.10 0.01 –0.50	pl cpx mt ol	60 5 8 2	Equant timag. and ilmenite. Some timag. have ilmenite exsolution. Pyrite and chalcopyrite present.	6% altered, ol completely replaced by olive green smectite. Smectite has basal d= 14.48Å which splits to form two peaks, d=14.72 and d= 16.98Å after glycol. Mainly smectite A but trace of B and chlorite(?) also. Sector zoned cpx.	P,R2,S,K,M
microlitic, intergranular	0.05 –0.96 0.002–0.20 0.001–0.05 0.01 –0.20	pl cpx mt ol	46 16 12 7	Timag. in groundmass Olivine phenocrysts contain chromite.	6% altered, ol almost completely replaced by green smectite with iddingsite rims. Smectite has basal d=14.72Å which expands to 16.66Å after glycol. Smectite B only. Sector zoned cpx phenocrysts. Rare large ol have kink-bands.	X,T,M
microlitic, intergranular	0.02 –1.70 0.005–0.50 0.003–0.20 0.01 –0.50 0.03 –0.06	pl cpx mt ol il	44 22 7 5 <1	Timag. and ilmenite. Pyrite and chalcopyrite are present, and olivine phenocrysts contain chromite that is zoned to chrome-rich timag. on rims.	7% altered, ol altered to olive brown smectite on rims and cracks. Smectite has basal d=14.24Å and 15.22Å which expand to 14.72 and 17.31Å after glycol. Only smectite B and chlorite(?) are present. Rare large ol have kink-bands.	S,P,T,R2, S,K,M
intergranular	0.03 –0.50 0.005–0.50 0.03 –0.50 0.001–0.10 0.01 –0.34	pl cpx ol mt il	45 22 7 7 1		16% altered, ol altered to iddingsite and olive smectite on rims and cracks. Smectice has basal d=13.38Å and 14.48Å which expands to 14.72 and 16.66Å after glycol. Only chlorite(?) and smectite B are present. Phillipsite identified by XRD. Rare large ol have kink-bands.	

APPENDIX – *Continued*

				Phenocrysts & Microphenocrysts			Vesicles				Groundmass
Hole	Core-Section, Interval (cm)	Flow Unit	Rock Type	Mineral	Per cent	Average Size (mm)	Per cent	Size Range (mm)	Average Size (mm)	Shape	Per cent
433C	6-2, 76–79	3	Alkalic Basalt	pl	2	1.48	1	0.15–0.77	0.37	elliptical	98
	10-2, 46–54	4c	Olivine Tholeiite	ol	8	1.49	26	0.55–7.48	2.58	irregular	92
	10-2, 136–143	4d	Tholeiite	ol	2	0.90	33	0.51–8.20	2.41	irregular-ovoid	98
	10-4, 11–17	4f	Tholeiite	ol	3	0.64	25	0.23–4.43	1.62	irregular-ovoid	97
	10-5, 84–90	5a	Tholeiite	ol	1	1.13	15	0.20–2.35	1.55	irregular	99
	11-1, 130–135	6	Tholeiite	ol	<1	0.72					99+
	11-3, 90–98	7	Tholeiite	ol	2	0.72					98
	12-1, 35–45	8	Olivine Tholeiite	ol pl cpx	5 3 1	1.49 0.65 0.61	20	0.51–5.80	3.26	ovoid-irregular	90+

APPENDIX – *Continued*

Groundmass						
Dominant Texture	Size Range (mm)	Minerals[a]	Per cent	Opaque Minerals	Alteration and Remarks[b]	Other Work
pilotaxitic	0.005–0.75 0.001–0.50 0.001–0.10 0.003–0.50 0.005–0.01 up to 0.01	pl cpx mt ol il ap	30–35 25–30 18–20 12–15 1–2 1		10–15% altered, ol completely replaced by smectite and iddingsite. Smectite has basal d=14.02Å which expands to 16.98Å after glycol. Only smectite B is present.	X,P,T,R2
ophitic-sub-ophitic	0.01 –0.55 0.01 –0.55 0.01 –0.48 0.001–0.01 0.01 –0.15	pl cpx ol mt il	43 37 7 4 1		42% altered, ol completely replaced by smectite and iddingsite. Pl mostly replaced by smectite and kf. Vesicles lined with fibrous pale green smectite. Smectite has basal d= 12.27 and 14.24Å which expands to 14.72 and 16.98Å after glycol. Smectite A, B and chlorite(?) are present. Some cpx is altered to amphibole(?).	
sub-ophitic	0.01 –1.22 0.01 –0.50 0.01 –0.50 0.005–0.10 0.01 –0.20	pl cpx ol mt il	55 27 10 4 3		22% altered, ol completely replaced by smectite and iddingsite. Pl is about half altered to smectite. Vesicles are lined with pale green fibrous smectite. Smectite has basal d= 13.59Å which expands to 16.66Å after glycol. Both smectite A and B are present. Some cpx altered to amphibole.	
sub-ophitic	0.01 –0.95 0.01 –0.20 0.01 –0.50 0.005–0.05 0.01 –0.16	pl cpx ol mt il	41 32 19 3 3	Exsolved skeletal timag. Olivine phenocrysts contain chromite that is zoned to chrome-rich timag. on rims. Single grain of magnesioferrite.	31% altered, ol completely replaced by smectite and iddingsite. Pl is about 50% replaced by smectite. Cpx is partly replaced by amphibole(?). Smectite has basal d=12.80Å which expands to 16.98Å after glycol. Mainly smectite B but trace of A also.	X,T,M
ophitic	0.01 –0.25 0.005–0.25 0.01 –0.50 0.005–0.10	pl cpx ol mt	50 40 5 4		43% altered, ol completely replaced by calcite, smectite, and iddingsite. Most vesicles are filled with fibrous yellow-green smectite. Smectite has basal d=12.80Å which expands to 17.66Å after glycol. Only smectite A present.	
ophitic	0.01 –0.60 0.01 –0.50 0.01 –0.50 0.01 –0.30 0.005–0.20	pl cpx ol il mt	53 31 13 2 <1		38% altered, ol completely replaced by calcite, smectite, and iddingsite. Smectite has basal d=12.62Å and 14.97Å (chlorite?) which expands to 17.31Å after glycol. Mainly smectite A, but trace of B also.	
sub-ophitic	0.02 –0.70 0.001–0.30 0.01 –0.50 0.005–0.25 0.001–0.05	pl cpx ol il mt	46 33 12 4 2		~36% altered, ol completely replaced by smectite and iddingsite. Smectite has basal d= 14.24 and 14.97Å (chlorite?) which expands to 16.98Å after glycol. Both smectite A and B present.	
intergranular	0.005–1.00 0.01 –0.50 0.01 –0.50 0.01 –0.25 0.005–0.05	pl cpx ol il mt	44 35 4 4 3		~40% altered, ol totally replaced by calcite, smectite, and iddingsite. Some pl cores altered to clays and kf(?). Vesicles lined with green fibrous smectite and calcite. Smectite has basal d=12.62Å which expands to 17.31Å after glycol. Only smectite A present.	

APPENDIX – *Continued*

				Phenocrysts & Microphenocrysts			Vesicles				Groundmass
Hole	Core-Section, Interval (cm)	Flow Unit	Rock Type	Mineral	Per cent	Average Size (mm)	Per cent	Size Range (mm)	Average Size (mm)	Shape	Per cent
433C	12-3, 57-65	9	Tholeiite	ol pl cpx	4 4 2	0.88 1.05 0.73	2	0.10-3.24	1.05	round-irregular	90
	13-2, 55-66	10	Plagioclase Tholeiite	pl cpx ol	13 4 1	1.28 0.91 0.77					81+
	14-3, 8-15	11c	Plagioclase Tholeiite	pl cpx	7 1	1.09 0.74	15	0.73-3.35	1.91	ovoid-irregular	93
	14-4, 18-24	11c	Plagioclase Tholeiite	pl cpx	9 2	0.87 0.82					89
	15-2, 58-64	11c	Plagioclase Tholeiite	pl cpx ol	6 1 <1	0.98 0.70 0.59	30	0.12-4.11	2.41	round-irregular	92
	15-4, 51-57	12	Tholeiite	pl ol cpx	1 <1 <1	0.54 0.45 0.57	23	0.05-5.63	1.17	irregular	98+
	15-6, 16-31	13	Tholeiite	pl cpx ol	1 1 <1	1.08 0.81 0.37					97+
	16-1, 106-110	13	Tholeiite	pl cpx	3 <1	1.01 0.68					96+
	17-1, 78-82	13	Tholeiite	pl cpx	2 1	1.16 0.76					97

APPENDIX – *Continued*

Groundmass						
Dominant Texture	Size Range (mm)	Minerals[a]	Per cent	Opaque Minerals	Alteration and Remarks[b]	Other Work
microlitic-intergranular	0.003–0.50 0.01 –1.10 0.01 –0.50 0.001–0.05 0.01 –0.05	cpx pl ol mt il	46 33 5 3 3	Tiny equant exsolved timag. Rare elongate crystals may be ilmenite.	16% altered, ol totally replaced by olive-green smectite and iddingsite. Smectite has basal *d*=12.80Å which splits to a *d*=14.72Å (chlorite?) and a 17.31Å peak after glycol. Only smectite A is present.	X,T,M
intergranular	0.05 –1.20 0.01 –0.50 0.05 –0.50 0.01 –0.70 0.005–0.26	pl cpx ol il mt	44 26 7 3 1	Equant exsolved timag. and elongate ilmenite. Pyrite is present.	25% altered, ol totally replaced by fibrous olive smectite. Smectite has basal *d*=13.38Å which splits to form two peaks, *d*= 14.48 and 16.66Å after glycol. Both smectite A and B, and chlorite(?) present. Pl phenocrysts contain glass inclusions.	X,T,R1,M
intergranular	0.01 –0.85 0.01 –0.50 0.01 –0.50 0.01 –0.20 0.001–0.05	pl cpx ol il mt	43 36 7 5 2	Skeletal exsolved timag. and elongate ilmenite.	21% altered, ol totally altered to smectite and iddingsite. Smectite has basal *d*=12.99Å which expands to 17.31Å after glycol. Only smectite A present. Vesicles lined with fibrous olive green smectite. Some pl cores are replaced by phillipsite(?) or kf.	X,T,R1,M
sub-ophitic	0.01 –0.72 0.01 –0.50 0.001–0.15 0.02 –0.20 0.01 –0.40	pl cpx mt ol il	48 31 6 2 2		23% altered, ol totally altered to smectite and iddingsite. Smectite has basal *d*=12.80Å which expands to 17.31Å after glycol. Only smectite A present. Some pl cores replaced by kf.	
intersertal	0.01 –0.60 0.01 –0.25 0.005–0.50 0.001–0.07 0.01 –0.43	pl cpx ol mt il	51 26 7 5 3		31% altered, ol totally altered to iddingsite and smectite. Smectite has basal *d*=13.59Å which expands to 17.31Å after glycol. Some vesicles filled with fibrous olive green smectite. Only smectite A is present.	
microlitic, subtrachytic	0.01 –0.50 0.001–0.50 0.001–0.05 0.005–0.05 0.01 –0.50	pl cpx mt il ol	50 37 8 3 1		40% altered, ol totally altered to smectite with iddingsite rims. Smectite has basal *d*= 12.80Å which expands to 17.31Å after glycol. Only smectite A is present. Most vesicles are filled with fibrous olive green smectite.	
subtrachytic, microlitic	0.005–0.65 0.001–0.50 0.001–0.10 0.01 –0.10 0.02 –0.35	pl cpx mt il ol	41 44 7 4 <1	Equant timag. with minor ilmenite exsolution and elongate ilmenite.	8% altered, ol totally altered to olive green-brown smectite and iddingsite. Smectite has basal *d*=12.62Å which expands to 18.02Å after glycol. Only smectite A is present.	W,X,T,S, K,M
microlitic, intergranular	0.01 –1.08 0.001–0.28 0.05 –0.20 0.001–0.10 0.01 –0.10	pl cpx ol mt il	52 34 5 3 2		4% altered, ol mostly altered to dark green-brown smectite. Smectite has basal *d*=14.02Å which expands to 16.98Å after glycol. Only smectite A is present. Rock is glomeroporphyritic.	
intergranular	0.01 –1.05 0.001–0.35 0.008–0.23 0.005–0.17 0.005–0.48	pl cpx il mt ol	50 40 4 2 1		2% altered, ol totally altered to dark green-brown smectite. Smectite has basal *d*= 14.72Å which splits to form two peaks, 14.72Å (chlorite?) and 16.98Å after glycol. Only smectite A is present.	W,X,P,R1, S,K

APPENDIX – *Continued*

				Phenocrysts & Microphenocrysts			Vesicles				Groundmass
Hole	Core-Section, Interval (cm)	Flow Unit	Rock Type	Mineral	Per cent	Average Size (mm)	Per cent	Size Range (mm)	Average Size (mm)	Shape	Per cent
433C	19-1, 35–42	13	Tholeiite	pl cpx	3 <1	1.23 1.05					96+
	19-2, 46–53	14	Plagioclase Tholeiite	pl cpx	6 <1	1.02 0.92					94
	19-5, 57–65	15a	Plagioclase Tholeiite	pl cpx ol	9 1 <1	1.42 1.20 1.24					90+
	21-1, 15–23	16	Tholeiite	pl ol	1 1	0.90 0.85	13	0.05–5.05	1.01	round-irregular	98+
	21-4, 7–13	17	Tholeiite	pl ol	1 1	0.93 0.80	24	0.09–7.18	1.79	round-irregular	98+
	22-5, 45–52	18	Plagioclase Tholeiite	pl ol	7 2	1.49 1.05	6	0.05–1.91	0.48	round-ovoid	91+
	23-1, 100–108	19a	Tholeiite	ol cpx	2 <1	1.23 0.68	18	0.05–4.00	0.88	irregular-branching	97+
	23-3, 111–119	19b	Tholeiitic Picrite	ol pl	28 1	1.46 0.49					70+

APPENDIX – *Continued*

Groundmass						
Dominant Texture	Size Range (mm)	Minerals[a]	Per cent	Opaque Minerals	Alteration and Remarks[b]	Other Work
sub-ophitic	0.005–1.00 0.01 –0.45 0.003–0.06 0.01 –0.43 0.005–0.07	pl cpx mt ol il	50 36 8 2 1		27% altered, ol totally altered to dark green-brown smectite and pleochroic iddingsite. Smectite has basal d=11.94Å which expands to 18.79Å after glycol. Only smectite A is present. Rock is glomero-porphyritic.	
sub-ophitic	0.01 –0.85 0.005–0.50 0.01 –0.50 0.005–0.10 0.01 –0.30	pl cpx ol mt il	42 42 5 3 2		35% altered, ol completely altered to olive-green smectite and iddingsite. Smectite has basal d=13.80Å which expands to 18.02Å after glycol. Only smectite A is present. Mt has hematite rims. Rock is glomeroporphyritic.	
sub-ophitic	0.02 –1.37 0.005–0.50 0.01 –0.42 0.005–0.17 0.01 –0.50	pl cpx il mt ol	47 40 2 1 <1	Equant skeletal timag. and ilmenite. Pyrite is present.	20% altered, ol totally altered to olive-green smectite and iddingsite. Smectite has basal d=12.99Å which expands to 17.66Å after glycol. Only smectite A is present. Rock is glomeroporphyritic.	X,T,R1,M
microlitic, intergranular	0.005–0.98 0.001–0.15 <0.001–0.09 0.003–0.50 0.008–0.15	pl cpx mt ol il	48 37 6 4 4		26% altered, ol totally altered to olive-green smectite and pleochroic iddingsite. Smectite has basal d=14.97Å which expands to 17.31Å after glycol. Only smectite A is present. Vesicles are filled with olive-green fibrous smectite.	
microlitic, intergranular	0.003–1.30 0.001–0.20 <0.001–0.10 0.008–0.20 0.01 –0.50	pl cpx mt il ol	45 40 7 5 <1	Titanomagnetite and elongate ilmenite. Timag. is flat gray in reflecting light indicating low-temp. oxidation. Pyrite is present.	25% altered, ol totally altered to olive-green smectite and iddingsite. Smectite has basal d=13.59Å which expands to 17.66Å after glycol. Smectite A and B and chlorite(?) present. Most vesicles are filled with fibrous olive-green smectite. Pl cores replaced by kf.	X,T,M
microlitic, intergranular	0.01 –0.95 0.001–0.10 <0.001–0.10 0.003–0.14 0.01 –0.50	pl cpx mt il ol	41 38 5 5 3	Equant timag. and elongate ilmenite. Olivine phenocrysts contain chromite. Pyrite is present.	17% altered, ol totally altered to olive-green smectite with iddingsite rims. Smectite has basal d=14.48Å which splits to form two peaks, 14.72Å (chlorite?) and 17.31Å, after glycol. Smectite A and B and chlorite (?) present. Vesicles filled with fibrous olive-green smectite.	X,T,R1,M
microlitic, intergranular	0.005–0.45 0.001–0.01 <0.001–0.02 0.01 –0.50 0.01 –0.06	pl cpx mt ol il	45 42 7 2 2		~20% altered, ol totally altered to olive-green fibrous smectite and iddingsite. Smectite has basal d=12.62Å which expands to 17.31Å after glycol. Only smectite A is present. Vesicles are almost all filled with fibrous olive-green smectite.	
sub-ophitic	0.01 –0.50 0.02 –0.75 0.01 –0.42 0.02 –0.50 0.003–0.15	cpx pl il ol mt	35 32 2 1 <1		46% altered, ol about half replaced by yellow to brown smectite with iddingsite rims. Smectite has basal d=14.72Å (chlorite?) and 16.35Å which shift to 14.72Å and 16.66Å after glycol. Smectite A and B and chlorite(?) present.	

APPENDIX – *Continued*

Hole	Core-Section, Interval (cm)	Flow Unit	Rock Type	Phenocrysts & Microphenocrysts: Mineral	Per cent	Average Size (mm)	Vesicles: Per cent	Size Range (mm)	Average Size (mm)	Shape	Groundmass: Per cent
433C	24-7, 133–139	19d	Tholeiitic Picrite	ol	36	1.93					64
	24-8, 9–10	19d	Tholeiitic Picrite	ol	23	2.02					77
	25-4, 13–16	21	Tholeiite	ol cpx	<1 <1	0.86 2.00	8	0.07–0.99	0.47	irregular	99+
	26-3, 79–87	21	Tholeiite	ol	<1	0.63	3	0.10–1.03	0.34	ovoid	99+
	27-2, 125–134	24a	Tholeiitic Picrite	ol	30	1.97					69+
	28-2, 73–80	25	Plagioclase Tholeiite	pl cpx	5 1	1.11 0.80	2	0.09–1.58	0.65	ovoid irregular	94+
	29-1, 112–113	26a	Plagioclase Tholeiite	pl cpx ol	5 1 <1	1.28 0.71 1.00	4	0.25–2.80	0.86	round-ovoid	94
	29-2, 94–100	26b	Plagioclase Tholeiite	pl cpx ol	7 1 1	1.40 0.95 1.08	3	0.05–2.35	0.72	irregular-round	91

APPENDIX – *Continued*

Groundmass						
Dominant Texture	Size Range (mm)	Minerals[a]	Per cent	Opaque Minerals	Alteration and Remarks[b]	Other Work
sub-ophitic	0.02 -1.00 0.01 -0.50 0.01 -0.40	pl cpx il	36 25 3	Equant timag. and elongate ilmenite. Olivine phenocrysts contain chromite. Pyrite is present.	37% altered, ol about 20–25% replaced by yellow smectite and rimmed by iddingsite. Smectite has basal d=14.72Å which splits to a 14.72Å and a 16.35Å peak after glycol. Smectite A, B, and chlorite are present. Mt partly replaced by hematite. Zeolites(?) present. Rare ol are kink-banded.	X,T,M
intergranular	0.01 -1.00 0.01 -0.40 0.15 -0.50 0.005-0.50	pl cpx ol il	39 25 11 2		38% altered, ol 10% replaced by bright blue-green and pale yellow-buff smectite. Smectite has basal d=15.49Å which expands by 17.66Å after glycol. Smectite B, chlorite and phillipsite are present. Rare ol are kink-banded.	
microlitic, intergranular	0.01 -0.66 <0.001-0.15 <0.001-0.15 0.01 -0.50 0.005-0.19	pl cpx mt ol il	50 37 7 5 1		18% altered, ol almost totally replaced by buff smectite and iddingsite rims. Smectite has basal d=13.59Å which expands to 17.66Å after glycol. Only smectite A is present. Vesicles filled with yellow to yellow-green fibrous smectite. Pl cores partly replaced by K-spar.	
intergranular	0.001-1.05 0.001-0.30 0.001-0.05 0.01 -0.50 0.005-0.10	pl cpx mt ol il	45 42 6 5 1		~12% altered, ol totally replaced by olive-green fibrous smectite and rimmed by iddingsite. Smectite has basal d= 13.59Å which expands to 18.39Å after glycol. Smectite A is present. Vesicles filled with olive-green fibrous smectite.	
sub-ophitic	0.005-1.20 0.01 -0.50 0.01 -0.50 <0.001-0.05	pl cpx ol mt	28 26 12 3		~59% altered, ol partly altered to fibrous buff smectite and iddingsite. Smectite has basal d=14.97Å which splits to a 14.72Å and a 17.66Å peak after glycol. Smectite B and chlorite present. Calcite in vein.	
intergranular	0.005-1.00 0.005-0.30 0.01 -0.20 0.003-0.20	pl cpx il mt	47 45 2 <1	Equant timag. and rare elongate ilmenite.	~3% altered, smectite has basal d=13.80Å which expands to 17.66Å after glycol. Smectite A is present. Rare phillipsite(?) also present. Vesicles are filled with brown smectite with green smectite at the center.	X,P,R1,S, K,M
intergranular	0.005-0.80 0.001-0.50 0.01 -0.37 0.005-0.10 0.01 -0.50	pl cpx il mt ol	45 40 5 2 2	Elongate ilmenite. Pyrite is present.	13% altered, ol completely altered to olive-green fibrous smectite and iddingsite. Smectite has basal d=13.80Å which expands to 17.31Å after glycol. Smectite A is present. Pl cores partly replaced by K-spar. Vesicles have thin lining of olive-green fibrous smectite.	X,T,R1,M
intergranular	0.005-1.66 <0.001-0.50 <0.001-0.05 0.01 -0.05 0.01 -0.50	ol cpx mt il ol	46 39 3 2 1	Tiny exsolved timag. and ilmenite. Olivine phenocrysts enclose chromite. Pyrite is present.	14% altered, ol totally altered to fibrous olive-green smectite with iddingsite rims. Smectite has basal d=12.80Å which expands to 17.31Å after glycol. Celadonite (d=10.04Å), smectite A, rare alkali fel-spar and zeolites are present. Vesicles filled with yellow-green celadonite.	X,T,R1,S, K,M

APPENDIX – *Continued*

Hole	Core-Section, Interval (cm)	Flow Unit	Rock Type	Phenocrysts & Microphenocrysts			Vesicles				Groundmass
				Mineral	Per cent	Average Size (mm)	Per cent	Size Range (mm)	Average Size (mm)	Shape	Per cent
433C	31-1, 28-34	27	Plagioclase Olivine Tholeiite	pl ol	7 6	0.96 0.98					87
	31-4, 119-127	28b	Tholeiitic Picrite	ol	19	1.16	17	0.15-5.13	1.81	round-irregular	81
	32-5, 123-132	29	Olivine Tholeiite	ol	8	0.79	36	0.34-5.00	1.86	round-ovoid	92+
	33-3, 13-19	31	Tholeiitic Picrite	ol	34	1.36					66+
	34-2, 103-111	32b	Tholeiitic Picrite	ol pl	15 1	2.07 0.89					83+
	34-4, 102-109	34a	Olivine Tholeiite	ol pl	7 1	1.13 0.49	13	0.02-6.05	1.60	round-irregular	92
	34-7, 114-121	35	Olivine Tholeiite	ol pl cpx	10 3 <1	1.37 0.78 1.20	6	0.05-1.77	0.46	irregular-branching	86+
	35-7, 121-129	36b	Tholeiite	ol pl	2 <1	0.74 0.65	1	1.43-2.18	1.80	round-ovoid	97+

APPENDIX – *Continued*

Groundmass						
Dominant Texture	Size Range (mm)	Minerals[a]	Per cent	Opaque Minerals	Alteration and Remarks[b]	Other Work
intergranular	0.005–1.05 <0.001–0.23 0.005–0.19 0.01 –0.20 0.01 –0.50	pl cpx mt il ol	40 37 5 3 2	Equant timag. and rare elongate ilmenite. Chromite and pyrite are present but rare.	5% altered, ol 10–15% replaced by buff smectite. Smectite has basal *d*=14.72Å and 14.97Å which shift to 14.72Å and 17.31Å after glycol. Chlorite(?) and smectite B are present. Some ol poikilitically encloses pl.	X,P,R1,S, K,M
sub-ophitic	0.005–1.55 0.001–0.30 0.01 –0.50 0.005–0.10 0.01 –0.19	pl cpx ol mt il	41 22 10 6 2		~78% altered, ol totally replaced by fibrous yellow smectite and iddingsite. Pl about 80% replaced by pale olive-green smectite. Smectite has basal *d*=14.72Å which expands to 16.98Å after glycol. Calcite, chlorite(?), and smectite B present. Vesicles filled with calcite and fibrous smectite.	
sub-ophitic	0.01 –0.75 0.001–0.25 0.005–0.50 0.005–0.15 0.008–0.25	pl cpx ol mt il	47 29 11 3 3		67% altered, ol totally replaced by fibrous olive-green smectite and iddingsite. Pl about 70% replaced by green smectite in cores. Smectite has basal *d*= 14.02Å which expands to 17.31Å after glycol. Smectite A and B and chlorite(?) present. Vesicles filled with fibrous olive-green smectite.	
ophitic	0.01 –0.91 0.01 –0.50 0.01 –0.50 0.01 –0.35 0.005–0.15	pl cpx ol il mt	30 27 5 3 2		38% altered, ol about half replaced by pale yellow smectite and iddingsite. Smectite has basal *d*=14.72Å and 16.15Å which shift to 14.72Å and 16.98Å after glycol. Chlorite(?) and smectite B present.	
ophitic	0.02 –1.00 0.02 –0.50 0.01 –0.50 0.01 –0.35 0.003–0.15	pl cpx ol il mt	47 26 5 4 1	Equant exsolved timag. and elongate ilmenite. Olivine phenocrysts contain chromite. Pyrite is present.	36% altered, ol totally altered to smectite and iddingsite. Smectite has basal *d*=14.24Å and 15.22Å which shift to 17.31Å after glycol. Smectite A, B, chlorite, hematite, and goethite present. Some cpx replaced by yellow-brown amphibole(?).	X,T,M
intergranular	<0.001–0.005 0.005–0.84 0.008–0.25 0.01 –0.50 <0.001–0.10	cpx pl il ol mt	40–50 35–40 7–8 5–7 2–3		~22% altered, ol totally replaced by pale-green to buff smectite and iddingsite. Pl cores replaced by pale smectite. Smectite has basal *d*=12.80Å which expands to 17.31Å after glycol. Calcite, phillipsite, amphibole, and smectite A are present.	
intergranular	0.01 –0.90 <0.001–0.20 0.001–0.15 0.01 –0.50 0.005–0.20	pl cpx mt ol il	44 36 4 2 <1	Tiny equant exsolved timag. and elongate ilmenite. Olivine phenocrysts contain chromite that is zoned to chrome-rich timag. Pyrite is present.	23% altered. Ol totally replaced by smectite and iddingsite. Smectite has basal *d*=12.80Å which expands to 17.31Å after glycol. Vesicles filled with fibrous pale olive-green smectite. Smectite A and rare carbonate present.	X,T,R1,M
sub-ophitic	0.05 –1.20 0.05 –0.50 0.03 –0.50 0.03 –0.55 0.01 –0.15	pl cpx ol il mt	47 36 7 5 1		37% altered. Ol completely altered to fibrous olive-green smectite and iddingsite. Smectite has basal *d*=12.44Å which expands to 17.31Å after glycol. Vesicles are filled with yellow-green to olive-green smectite. Smectite A is present.	

APPENDIX – *Continued*

Hole	Core-Section, Interval (cm)	Flow Unit	Rock Type	Phenocrysts & Microphenocrysts			Vesicles				Groundmass
				Mineral	Per cent	Average Size (mm)	Per cent	Size Range (mm)	Average Size (mm)	Shape	Per cent
433C	36-4, 138–148	40	Olivine Tholeiite	ol	7	1.24	9	0.65–5.23	2.03	round-irregular	93
	37-3, 79–87	44	Tholeiite	ol	2	0.75					98
	38-1, 67–76	45b	Olivine Tholeiite	ol	9	1.10					91
	38-5, 85–93	47a	Tholeiite	ol	1	0.60					99+
	39-5, 87–94	48	Olivine Tholeiite	ol	5	1.21					95
	40-2, 88–96	49	Olivine Tholeiite	ol	8	1.43					92
	41-1, 40–49	51b	Tholeiite	pl cpx	2 1	0.84 0.60					97
	41-4, 51–58	51b	Tholeiite	pl	1	1.04					99
	42-1, 56–63	52	Tholeiite	ol pl cpx	1 <1 <1	0.78 1.16 0.67					99

APPENDIX – *Continued*

Groundmass						
Dominant Texture	Size Range (mm)	Minerals[a]	Per cent	Opaque Minerals	Alteration and Remarks[b]	Other Work
sub-ophitic	0.01 –0.85	pl	45		45% altered. Ol totally replaced by fibrous yellow-green smectite with iddingsite rims. Smectite has basal d=12.80Å which expands to 17.31Å after glycol. Vesicles are lined or filled with fibrous celadonite (d=9.93Å) and smectite. Rare amphibole(?) replacing cpx. Smectite A only.	
	0.01 –0.41	cpx	38			
	0.01 –0.50	ol	4			
	–	mt	3			
	–	il	3			
sub-ophitic	0.03 –1.35	pl	57	Equant to skeletal timag. and elongate ilmenite. Olivine phenocrysts contain chromite.	18% altered. Ol totally replaced by fibrous olive green smectite and iddingsite. Smectite has basal d=14.24Å which expands to 17.31Å after glycol. Smectite A, B, and chlorite(?) present.	X,T,M
	0.02 –0.50	cpx	32			
	0.05 –0.50	ol	4			
	0.05 –0.50	il	4			
	0.01 –0.34	mt	1			
ophitic	0.01 –0.65	pl	50	Elongate ilmenite. Olivine phenocrysts contain chromite that is zoned to chrome-rich timag. Pyrite is present.	31% altered. Ol about 20% altered to pale yellow fibrous smectite with fibrous yellow-deep green and bright blue-green (pleochroic) smectite along fractures and rims. Smectite has basal d=14.72Å which splits to form a 14.72Å and a 17.66Å peak after glycol. Chlorite(?), smectite B, and phillipsite are present.	X,T,M
	0.01 –0.50	cpx	33			
	0.01 –0.50	ol	5			
	0.01 –0.42	il	3			
	0.001–0.12	mt	1			
ophitic	0.01 –1.35	pl	54		37% altered. Ol totally replaced by fibrous buff-green smectite and iddingsite. Smectite has basal d=14.48Å which expands to 16.66Å after glycol. Smectite A, B, and chlorite(?) present.	
	0.01 –0.50	cpx	31			
	0.01 –0.50	ol	10			
	0.01 –0.45	il	5			
intergranular	0.02 –0.50	pl	47	Elongate ilmenite. Olivine phenocrysts contain chromite that is zoned to chrome-rich timag. Some ilmenites are exsolved.	18% altered. Ol about 80% altered to smectite, chlorite, and iddingsite. Smectite has basal d=14.78Å and 14.98Å which shift to 14.72Å and 17.31Å after glycol. Smectite B and chlorite present.	X,T,R1,M
	0.005–0.50	cpx	37			
	0.005–0.50	ol	8			
	0.01 –0.35	il	2			
	0.003–0.19	mt	1			
intergranular	0.01 –0.45	pl	41	Elongate ilmenite; many are mottled because of a combination of high- and low-temp. oxidation. Olivine phenocrysts contain chromite. Nearly pure magnetite pyrite, and chalcopyrite are present.	19% altered, ol about 30% altered to smectite, chlorite, and iddingsite. Smectite has basal d=14.78Å and 14.98Å which shifts to 14.72Å and 16.66Å after glycol. Smectite B and chlorite present.	X,P,T,R1,M
	0.001–0.25	cpx	38			
	0.05 –0.50	ol	8			
	0.005–0.25	il	3			
	0.001–0.20	mt	2			
intergranular	0.01 –1.65	pl	50		23% altered. Smectite has basal d=12.27Å which expands to 17.31Å after glycol. Smectite A only. Hematite after some mt.	
	0.01 –0.50	cpx	40			
	0.008–0.15	mt	3			
	0.01 –0.70	il	3			
	0.05 –0.50	ol	1			
intergranular	0.01 –1.25	pl	60		31% altered. Smectite has basal d=12.62Å which expands to 17.31Å after glycol. Smectite A only. Hematite after some mt.	
	0.01 –0.50	cpx	29			
	0.01 –0.40	il	6			
	0.005–0.15	mt	3			
	0.05 –0.50	ol	1			
intergranular	0.01 –1.85	pl	53	Equant exsolved timag. and elongate ilmenite. Pyrite is present.	~23% altered. Ol totally altered to bright blue-green fibrous smectite and iddingsite. Smectite has basal d= 12.62Å which expands to 17.31Å after glycol. Smectite A only. Rare amphibole(?) after clinopyroxene.	S,T,R1,M
	0.01 –0.50	cpx	37			
	0.01 –0.67	il	4			
	0.05 –0.50	ol	3			
	0.005–0.30	mt	2			

APPENDIX – *Continued*

Hole	Core-Section, Interval (cm)	Flow Unit	Rock Type	Phenocrysts & Microphenocrysts			Vesicles				Groundmass
				Mineral	Per cent	Average Size (mm)	Per cent	Size Range (mm)	Average Size (mm)	Shape	Per cent
	42-3, 11–20	53	Plagioclase Tholeiite	pl cpx ol	17 4 1	1.61 1.25 0.85					77+
	42-5, 85–90	54	Plagioclase Tholeiite	pl ol cpx	14 1 1	1.89 1.04 1.34					84
433C	44-1, 31–35	56	Olivine Tholeiite	ol pl cpx	7 <1 <1	0.85 0.74 0.48					92
	44-4, 74–81	58	Tholeiite	pl cpx	1 1	0.85 0.78	1	0.35–1.41	1.11	round	97+
	45-2, 26–33	59c	Tholeiite	pl cpx	2 1	0.84 0.73					97
	45-5, 96–104	60	Plagioclase Tholeiite	pl cpx ol	8 1 1	1.59 1.03 0.73					89+
	45-8, 3–9	61a	Tholeiite	pl cpx ol	3 1 <1	1.29 1.43 0.78					96
	46-3, 43–51	62a	Tholeiite	pl cpx ol	4 1 1	1.17 0.81 0.74					93+
	47-5, 92–100	64	Tholeiite	ol pl	2 1	1.39 1.05	11	0.02–3.38	0.71	irregular	97

APPENDIX – *Continued*

	Groundmass					
Dominant Texture	Size Range (mm)	Minerals[a]	Per cent	Opaque Minerals	Alteration and Remarks[b]	Other Work
intergranular	0.01 -1.80 0.005-0.50 0.05 -0.50 0.01 -0.51 0.005-0.39	pl cpx ol il mt	46 26 2 2 1	Skeletal timag. and elongate ilmenite. Pyrite is present.	24% altered. Rounded embayed ol totally altered to fibrous olive-green smectite and iddingsite. Smectite has basal d=12.80Å which expands to 17.31Å after glycol. Smectite A only.	X,T,R1,M
intergranular	0.005-1.11 0.01 -0.50 0.01 -0.55 0.01 -0.50 0.005-0.30	pl cpx il ol mt	42 35 4 2 1	Equant exsolved timag. and elongate ilmenite. Olivine contains rare chromite.	12% altered. Rounded embayed ol totally altered to bright blue-green fibrous smectite and iddingsite. Smectite has basal d=12.44Å which expands to 17.31Å after glycol. Smectite A only.	X,T,R1,M
sub-ophitic	0.01 -1.34 0.05 -0.50 0.01 -0.90 0.005-0.25 0.05 -0.50	pl cpx il mt ol	47 37 4 3 <1		24% altered. Ol totally altered to fibrous olive-green smectite and iddingsite. Smectite has basal d=12.80Å which expands to 17.31Å after glycol. Smectite A only.	
intergranular	0.01 -1.19 0.005-0.50 0.01 -0.35 0.005-0.15 0.01 -0.50	pl cpx il mt ol	53 35 6 2 1		23% altered. Vesicles filled or lined with fibrous yellow-brown to olive-green smectite. Smectite has basal d=13.59Å which expands to 17.31Å after glycol. Smectite A only.	
intergranular	0.01 -1.37 0.005-0.50 0.01 -0.43 0.003-0.20 0.01 -0.50	pl cpx il mt ol	50 40 4 2 1		22% altered. Groundmass ol totally altered to smectite, celadonite, and iddingsite. Smectite has basal d=13.66Å which expands to 17.66Å after glycol. Smectite A and celadonite (d=10.04Å) present. Hematite replaces some mt.	
intergranular	0.01 -1.30 0.01 -0.50 0.02 -0.60 0.05 -0.50 0.01 -0.25	pl cpx il ol mt	48 22 4 3 2		~15% altered, ol totally altered to olive-green smectite and iddingsite. Smectite has basal d=14.72Å which expands to 16.98Å after glycol. Smectite A only.	
intergranular	0.01 -1.25 0.005-0.50 0.03 -0.50 0.03 -0.40 0.005-0.12	pl cpx ol il mt	58 32 4 1 1		23% altered, ol totally altered to smectite, celadonite, and iddingsite. Smectite has basal d=14.24Å which expands to 17.31Å after glycol. Smectite A and celadonite (d=10.04Å) present. Rare alkali feldspar in groundmass.	
intergranular	0.01 -1.03 0.01 -0.50 0.06 -0.50 0.02 -0.37 0.005-0.20	pl cpx ol il mt	56 29 3 3 2		30% altered. Ol totally altered to iddingsite and minor smectite and celadonite (d=10.04Å). Smectite has basal d=12.99Å which expands to 17.31Å after glycol. Smectite A only. Alkali feldspar replaces some pl cores.	
microlitic intergranular	<0.001-0.13 0.005-0.87 <0.001-0.15 <0.001-0.50 0.005-0.19	cpx pl mt ol il	40-45 30-35 7-10 5-7 1-2	Tiny equant exsolved timag. Olivine contains rare chromite. Pyrite is present.	20-23% altered. Ol totally altered to iddingsite. No clays detected. Vesicles filled with phillipsite and rare smectite. Phillipsite also replaces some pl.	X,T,R1,M

APPENDIX – *Continued*

Hole	Core-Section, Interval (cm)	Flow Unit	Rock Type	Phenocrysts & Microphenocrysts: Mineral	Per cent	Average Size (mm)	Vesicles: Per cent	Size Range (mm)	Average Size (mm)	Shape	Groundmass: Per cent
433C	48-3, 144–150	65a	Tholeiite	ol	1	0.83	17	0.41–4.05	1.63	ovoid-irregular	97+
				pl	1	0.69					
	49-2, 17–24	66	Tholeiite	pl	2	0.87					96
				ol	1	0.76					
				cpx	1	0.78					

Note: pl = plagioclase; ol = olivine; cpx = clinopyroxene; il = ilmenite; mt = magnetite; ap = apatite; kf = potash feldspar.

[a]By modal analysis of stained thin sections. Magnetite distinguished from ilmenite by shape. All percentages corrected for low-temperature alteration.

[b]Smectite A is expandable on glycolation. Smectite B is only partially expandable on glycolation. Chlorite is not expandable.

Other Work:
- W = wet chemical analysis
- X = X-ray fluorescence for majors
- P = microprobe for majors (Bence, et al.)
- T = X-ray fluorescence for trace elements
- R1 = INAA for rare earths and trace elements (Clague & Frey)
- R2 = ES for rare earths and trace elements (Bence, et al.)
- S = Sr isotopic analysis (Lamphere, et al.)
- K = K-Ar ages (Dalrymple et al.)
- M = microprobe mineral analyses (Clague, et al.)

APPENDIX – *Continued*

Groundmass						
Dominant Texture	Size Range (mm)	Minerals[a]	Per cent	Opaque Minerals	Alteration and Remarks[b]	Other Work
intersertal	0.02 –1.32 0.02 –1.35 0.01 –0.50 0.005–0.05 0.01 –0.50	pl cpx ol mt il	51 32 11 2 1		24% altered. Ol totally altered to iddingsite and smectite. Smectite has basal d=13.38Å that expands to 17.31Å after glycol. Smectite A only. Vesicles lined with pale yellow-green fibrous smectite. Much of the groundmass stains yellow with sodium cobaltnitrite.	
intersertal	0.02 –1.20 0.02 –0.50 0.01 –0.50 0.01 –0.85 0.005–0.55 –	pl cpx ol il mt kf	60 17 12 6 1 1	Equant rarely exsolved timag. and elongate ilmenite. Olivine contains rare chromite. Pyrite is present.	~27% altered. Ol totally altered to iddingsite and smectite. Smectite has basal d= 12.62Å which expands to 17.31Å after glycol. Many pl cores replaced by kf. Phillipsite and amphibole(?) after clinopyroxene are also present.	X,T,R1,M